Journal of Physiology (2002), **543.1**, *pp.* 49–70
DOI: 10.1113/jphysiol.2002.018465

www.jphysiol.org

Journal of Physiology

-Dynamic representation of whisker deflection by synaptic potentials in spiny stellate and pyramidal cells in the barrels and septa of layer 4 rat somatosensory cortex

Michael Brecht and Bert Sakmann

Abteilung Zellphysiologie, Max-Planck Institut für medizinische Forschung, Heidelberg, Germany

Whole-cell voltage recordings were made *in vivo* from excitatory neurons ($n = 23$) in layer 4 of the barrel cortex in urethane-anaesthetised rats. Their receptive fields (RFs) for a brief whisker deflection were mapped, the position of the cell soma relative to barrel borders was determined for 15 cells and dendritic and axonal arbors were reconstructed for all cells. Three classes of neurons were identified: spiny stellate cells and pyramidal cells located in barrels and pyramidal cells located in septa. Dendritic and, with some exceptions, axonal arborisations of barrel cells were mostly restricted to the borders of a column with a cross sectional area of a barrel, defining a cytoarchitectonic barrel-column. Dendrites and axons of septum cells, in contrast, mostly extended across barrel borders. The subthreshold RFs measured by evoked postsynaptic potentials (PSPs) comprised a principal whisker (PW) and several surround whiskers (SuWs) indicating that deflection of a single whisker is represented in multiple barrels and septa. Barrel cells responded with larger depolarisation to stimulation of the PW (13.7 ± 4.6 mV (mean ± S.D.), $n = 10$) than septum cells (5.7 ± 2.4 mV, $n = 5$), the gradient between peak responses to PW and SuW deflection was steeper and the latency of depolarisation onset was shorter (8 ± 1.4 ms *vs.* 11 ± 2 ms). In barrel cells the response onset and the peak to SuW deflection was delayed depending on the distance to the PW thus indicating that the spatial representation of a single whisker deflection in the barrel map is dynamic and varies on the scale of milliseconds to tens of milliseconds. Septum cells responded later and with comparable latencies to PW and SuW stimulation. Spontaneous (0.053 ± 0.12 action potentials (APs) s^{-1}) and evoked APs (0.14 ± 0.29 APs per principal whisker (PW) stimulus) were sparse. We conclude that PSPs in ensembles of barrel cells represent dynamically the deflection of a single whisker with high temporal and spatial acuity, initially by the excitation in a single PW-barrel followed by multi-barrel excitation. This presumably reflects the divergence of thalamocortical projections to different barrels. Septum cell PSPs preferably represent multiple whisker deflections, but less dynamically and with less spatial acuity.

(Received 6 February 2002; accepted after revision 24 May 2002)
Corresponding author M. Brecht: Max-Planck Institut für medizinische Forschung, Abteilung Zellphysiologie, Jahnstraße 29, D-69120 Heidelberg, Germany. Email: brecht@mpimf-heidelberg.mpg.de

The elaborate morphology of cortical neurons has been established for a long time (Ramon y Cajal, 1893), yet the functional significance of the differences in the architecture of the dendritic and axonal arbors of cells located in the same or different cortical layers is still unclear. Layer 4 of rodent somatosensory cortex is divided cytoarchitectonically into barrels with a high density of neurons, and septa between barrels with a lower density (Woolsey & Van der Loos, 1970). Barrel cells are targeted by thalamic inputs from the ventral posterior medial nucleus (VPM; for review see Diamond, 1995) while septum cells are innervated by thalamic afferents projecting from the posterior medial nucleus (PoM; for review see Kim & Ebner, 1999). A functional equivalent of the cyto-architectonically defined barrels are the barrel-columns, ensembles of cells in the different cortical layers which share functional properties such as a response preference for the deflection of a particular whisker. The receptive fields (RFs) of barrel-column cells are characterised by a dominant input from a principal whisker (PW) and weaker inputs from surround whiskers (SuW). In L4 the barrel-columns correspond in their dimensions roughly to barrels (Welker, 1976). Barrel borders can be visualised simultaneously with the dendritic morphology of individual cells (Ito, 1992), and both the laminar location of a cell's soma and the spread of dendrites and axon collaterals can be determined relative to the barrel borders. Thus possible anatomical determinants of RF structure, such as the geometry of the dendritic and axonal arbor can be delineated.

Spiny stellate cells are confined to the borders of barrels and their dendritic arbor is asymmetric (Woolsey *et al.* 1975; Simons & Woolsey 1984; Feldmeyer *et al.* 1999; Lübke *et al.* 2000). They relay thalamic output to other cortical layers via axon collaterals projecting to L2/3 and to L5 or L6. Although most anatomical studies on L4 neurons have focused on spiny stellate cells, pyramidal neurons have also been described in somatosensory (Lorente de No, 1922; Elston *et al.* 1997; Lübke *et al.* 2000) and in visual cortex (Martin & Whitteridge, 1984). In the somatosensory cortex neurons in layer 4 are selective in their responses to the direction of whisker deflection and they respond with short latency. Their RF structure is somewhat controversial, however. Intracellular recordings with microelectrodes (Carvel & Simons, 1988) and more recently, whole-cell voltage recordings have demonstrated afferent inputs from several whiskers and large subthreshold RFs (Moore & Nelson, 1998; Zhu & Connors, 1999). Most (Simons, 1995) but not all (Armstrong-James, 1995) extracellular unit-recording studies report small, often single-whisker RFs. In addition multielectrode unit recordings indicate that RF properties are time dependent (Petersen & Diamond, 2000).

We report *in vivo* whole-cell voltage recordings combined with morphological reconstruction of the recorded neurons and determination of their columnar position. The aim was to establish firstly the dependency of RF structure on the geometry of dendritic and axonal arborisation of the different classes of neurons to identify possible constraints of RF structure given by cell morphology. Secondly we wanted to determine possible relationships between a cell's location and morphology and the time dependent structure of sub- and suprathreshold RFs. Such relations are essential to elucidate how different tactile object cues are represented at the input (PSPs) and the output stage (APs) of specific ensembles of cells in the cortical input layer.

METHODS

The methods employed have been described in detail elsewhere (Brecht & Sakmann, 2002) and thus the description will be limited.

Animals

Forty-eight Wistar rats of both sexes were used. The animals were between 28 and 36 days old. In 43 animals at least one cell was recorded. However not all of these cells could be recovered for reconstruction, and not all of the recovered cells were located in L4.

Preparation

Animals were prepared as described previously. In brief, rats were anaesthetised with an intraperitoneal injection of urethane (1–1.5 g kg^{-1}). A 1 mm diameter hole in the skull was drilled at 5.5 mm lateral and 2.5 mm posterior to bregma. The dura was removed with a 30 gauge injection needle tip and the exposed cortex was superfused with warm Hepes buffered artificial cerebrospinal fluid (ACSF) solution. All experimental procedures were carried out according to the animal welfare guidelines of the Max-Planck Society.

Anaesthesia

Depth of anaesthesia was assessed by monitoring pinch withdrawal, eyelid reflex, corneal reflex, respiration rate and vibrissae movements. In the recording conditions chosen here, pinch withdrawal and vibrissae movements were usually absent, but weak eyelid and corneal reflexes could be observed. Respiration rates were usually between 70–100 breaths min^{-1}. During the whole experiment animals were anaesthetised with urethane, the depth of anaesthesia during recordings generally being lower than during the initial surgery. Occasionally, both vibrissae movements and withdrawal reflexes began to appear during the course of the experiment. In these cases an additional dose urethane (20 % of the initial dose) was given. Taken together, these observations suggest that the depth of anaesthesia varied in our animals around anaesthetic state III-3 (Friedberg *et al.* 1999).

Whole-cell recording

Recordings were made with long taper patch pipettes with DC-resistances of 4–7 MΩ pulled from borosilicate glass tubing on a Sutter puller (Science Products, Hofheim, Germany) in a three-stage pull. Pipettes were filled with (mM): potassium gluconate 130, sodium gluconate 10, Hepes 10, phosphocreatine 10, MgATP 4, Na_2ATP 2, GTP 0.3, NaCl 4 and 0.4 % biocytin at pH 7.2.

Pipettes were lowered perpendicularly to the cortical surface into the barrel cortex. To prevent tip occlusion during passage to L4 pressure (200–300 mbar) was applied to the pipette interior. To establish the whole-cell recording configuration we applied conventional voltage-clamp (Blanton *et al.* 1989; Margrie, Brecht & Sakmann, 2002). Series resistances were between 10 and 80 MΩ. All data have been corrected for a +7 mV junction potential.

Sensory stimulation and receptive fields

A piezoelectric bimorph wafer with an attached glass capillary served for quantitative single whisker stimulation (Simons, 1983). Steps elicited by the piezoelectric device had a 10–90 % rise time of 1 ms. The deflection point of the whisker was chosen to be 8–10 mm from the base of the vibrissa and if not otherwise noted the vibrissa was deflected backwards for 1 mm (roughly 6 deg deflection angle) for 200 ms. Airpuffs were generated from pulses of compressed air, delivered in a computer controlled way by a picospritzer unit (General Valve Corporation, Fairfield, USA). Airpuffs were applied through a stiff micropipettor tip with a 2 mm opening positioned 10–15 mm rostrolateral from the whiskers. Under these conditions the airpuff stimuli deflected 4–8 whiskers in two to three whisker rows by up to 2 mm. The airpuff stimulus was moved across the whisker array and 20 airpuff stimuli were applied at the most effective position.

Cells entered our sample only if at least 10 whiskers had been mapped. For repetitive stimulation we applied brief (2 ms) back and forth deflections (6 deg). For PSP latency measurements we determined the latency from stimulus onset to where the postsynaptic potential reached 5 % of its peak amplitude. AP latency was measured as the time after whisker deflection onset to the peak of the AP. If not noted otherwise, median values of latencies are given.

To quantify the direction tuning of various response components a directionality index was calculated as follows: (response in the

preferred direction – response in the opposite direction)/(response in the preferred direction + response in the opposite direction). Thus, values of 1 represent completely directional responses, values of 0 represent completely non-directional responses. In our data set this measure of response directionality leads to qualitatively and quantitatively similar results to a directionality index based on all deflection directions (data not shown).

Histological procedures and reconstruction

On the completion of physiological recordings animals were perfused transcardially (when necessary after an additional dose of urethane) with 0.1 M phosphate-buffered saline (PBS) followed by a solution of 4% paraformaldehyde. The brain was removed from the skull and immersed in fixative for at least 1 day and then it was sectioned in 100 or 300 μm thick slices. Two planes of section were used. From a few brains tangential sections of barrel cortex were prepared. For a majority of brains the semicoronal plane of section was chosen. Here the plane of section was perpendicular to the cortical surface and tilted 45 deg away from the coronal plane towards the sagittal plane, whereby the section ran from anterior for the medial part of the brain to posterior for the lateral part. This angle of the section resulted in a cut perpendicular to rows of barrels and parallel to arcs of barrels. For simplicity we refer to these sections as 'coronal' sections. In most slices, cytochrome oxidase staining (Wong-Riley, 1979) was used to visualise the cortical layering and barrel structure. Slices were then processed with the avidin-biotin-peroxidase method (Horikawa & Armstrong, 1988) to reveal cell morphology and mounted on slides using moviol. Subsequently biocytin labelled neurons were reconstructed with Neurolucida software (Microbrightfield, Colchester, VT, USA) using a Zeiss Axioplan microscope fitted with a 40 × objective. Reconstruction resulted in three-dimensional cell morphology. Most cells appeared to be artificially flattened in the *z*-axis during staining and embedding and in these cells the analysis of dendritic field geometry was restricted to two-dimensional semicoronal or horizontal projections. However, in a subset of cells the *z*-shrinkage was negligible, and these cells ($n = 7$) are shown in both semicoronal and horizontal projections. The soma diameter was calculated as the mean of the maximum and the minimum soma diameter. For density plots (see below), where cells are represented relative to barrel borders, we have aligned them to an averaged barrel pattern, derived from four brains (horizontal sections) and five brains (coronal sections), in which barrel outlines could be clearly delineated.

Subpial depth and identification of L4 cells

The micromanipulator angle (*ca* 35 deg tilt away from the vertical axis) was adjusted to allow a perpendicular penetration through cortical layers. The somata of recovered cells were found to reside at a depth of 0–250 μm less than the read-out of the micromanipulator, suggesting firstly that with our type of pipette we did not record from apical dendrites. Contrary to our observation, such recordings should have led to a recovery of cell somata at a depth in excess of the micromanipulator reading. Second, there appear to exist systematic errors that bias the micromanipulator depth estimate towards too high values. Such errors may include an imperfectly perpendicular penetration, tissue compression by the pipette and an incorrect estimate of the pia position due to the fluid level on the surface of the brain. Given the fact that the depth underestimation from micromanipulator read out almost matches the thickness of L4 we did not include non-identified cells in the L4 sample. L4 was identified either by granular appearance in unstained tissue sections, or by a brown appearance in the cytochrome C stained section. The most superficial L4 cell was encountered at a subpial depth of 595 μm (as indicated by the micromanipulator read-out). The deepest recording resulting in the recovery of a L3 cell was done at a manipulator depth of 799 μm. Between 600–700 μm a few L4 cells were identified but a majority of cells at that depth were located in L2/3. Between 700–800 μm depth both L2/3 and L4 cells were identified, the identified L4 cells all being located in the upper part of L4. We estimate that the L3/L4 boundary was encountered at a depth of around 750 μm. Relatively few recordings were made at a depth between 850–1000 μm and our sample of L4 cells therefore stems mainly from the upper part of L4. Pyramidal cells in L5 were encountered at depth of 1000 μm or deeper.

Classification of cell morphology

All cells included in this report had dendritic spines. Given the low number of cells we chose a broad cell classification scheme. We distinguish between spiny stellate and pyramidal L4 cells. The defining criteria for spiny stellate cells used here was the presence of spines and that more than 80% of their dendrites were confined to L4. The cells classified this way were all very spiny, lacked a clear cut apical dendrite and their dendritic field was often strongly polarised. Pyramidal cells in contrast were less spiny and had a prominent apical dendrite extending into layer 2/3.

Plots of RFs and of dendritic and axonal densities

Smoothed RF plots were generated by linear interpolation. To generate 2D maps of dendritic and axonal length densities, cell reconstructions generated in Neurolucida were converted into a Neuron software format. With Neuron (Hines & Carnevale 1997) the total length of all dendrites or axons within voxels of 50 μm × 50 μm × 50 μm were calculated. The resulting 3D density matrix was projected onto either a tangential or vertical plane resulting in a 2D density matrix. This 2D density matrix was read into Mathematica software and was low-pass filtered by convolving it with a 2D Gaussian kernel with a standard deviation of 50 μm. A bicubic interpolation of the filtered 2D density matrix was performed to generate a 2D density map. For averaging dendritic and axonal arborisations across cells, reconstructions were aligned relative to the centre of the respective barrel or septum.

RESULTS

The 23 putatively excitatory L4 neurons responded with regular AP patterns upon current injection and their dendrites were covered with spines. Six spiny stellate cells and 17 pyramidal neurons were identified. Of the six spiny stellate cells, three were localised within a barrel whereas for three the outlines of barrels were not clearly identified. Seven of the pyramidal cells were located within a barrel and five cells were located in a septum.

The neurons recorded from had low rates of spontaneous AP activity, the average being 0.053 ± 0.12 AP s^{-1} (mean ± S.D.). In some cells the rate of spontaneous APs increased slightly during the course of the recording (usually lasting 20–40 min). The pattern of ongoing subthreshold activity was similar in all recorded neurons. It was characterised by alternating states of hyperpolarised membrane potentials (down-state) during which little or no synaptic background

Journal of Physiology

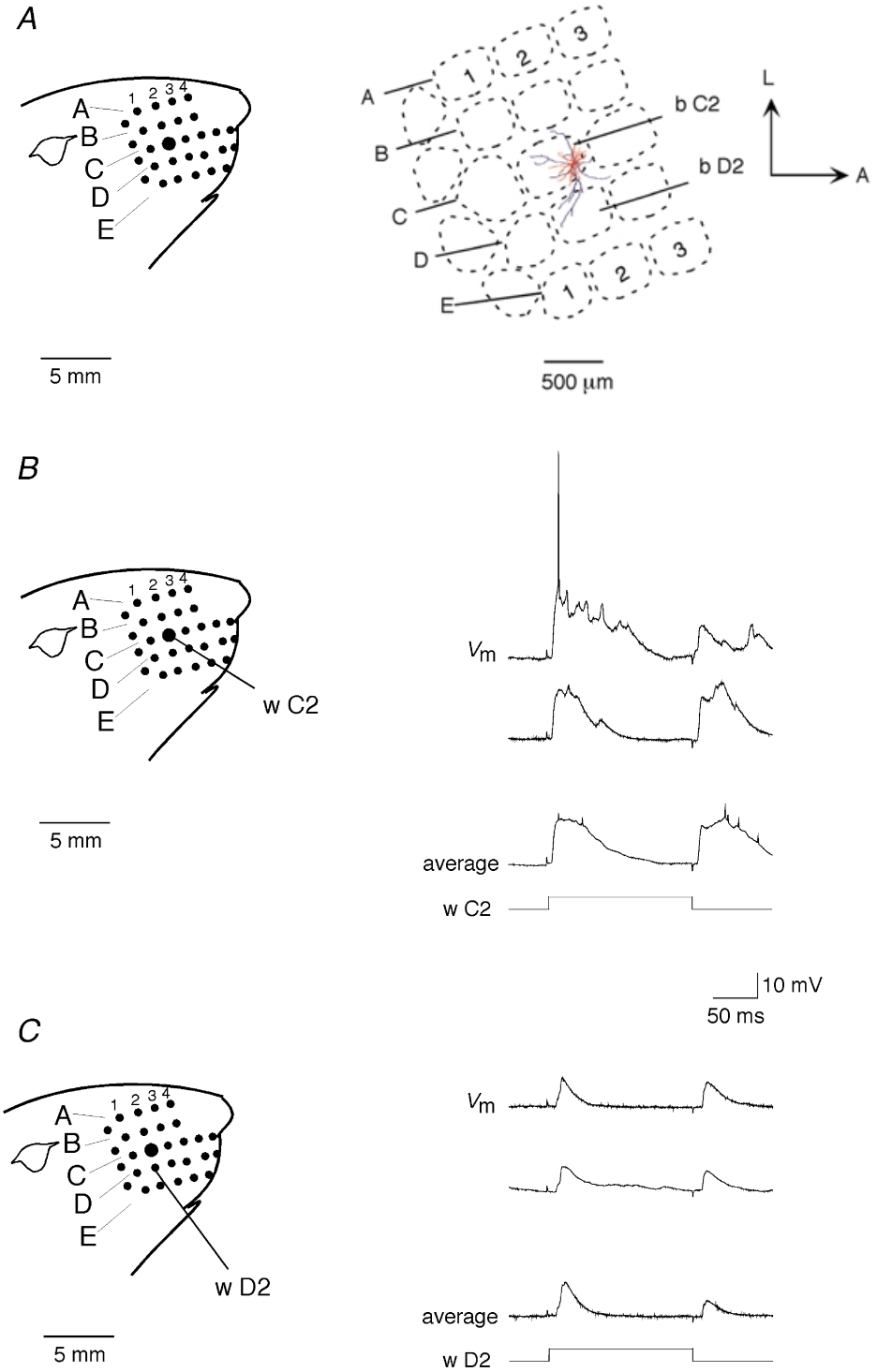

Figure 1. Position, morphology and sensory responses of a barrel spiny stellate cell

A, left panel shows a schematic representation of the whisker arrangement in the rat's right face. Right panel, schematic representation of the whisker barrel field of left hemisphere: A anterior, L lateral. The soma of reconstructed cell is located in the C2 barrel. Projection of dendritic (red) and axonal arbors (blue) onto the horizontal plane is shown relative to position of barrel borders (dashed lines); thickness of the axonal tracing has been slightly increased to improve visibility. *B*, left panel shows location of principal whisker (PW, wC2). Right panel illustrates two successive responses (V_m) to PW deflection evoking a PSP followed by an AP (upper trace) or a PSP (middle trace) at the deflection onset and offset respectively. The average response (20 trials) is shown in the lower trace. Time course of whisker deflection (wC2) is shown schematically below the records of membrane potential. *C*, stimulation of surround whisker (SuW, wD2): Two successive responses (V_m) to a surround whisker (wD2) deflection and averaged response (20 trials). Onset and offset stimulus artefacts are seen in all records as small upward deflections. The calibration bars apply to both *B* and *C*.

activity was observed and 10–20 mV more depolarised membrane states (up-state) during which synaptic background activity could be observed.

We will first describe the RF structure measured by response peak amplitudes for different cell classes and subsequently the time dependent response properties.

Receptive field structure of morphologically identified neurons in barrels and septa

All cells recorded from responded to deflection of multiple whiskers with membrane depolarisation. A division of RFs into excitatory and inhibitory whiskers was not evident. The depolarisation amplitude increased with deflection amplitude. All neurons, except one septum cell, responded with depolarisations in response to PW stimulation that exceeded 5 mV. Only 1 of 12 neurons tested also responded at short latency (< 100 ms) to stimulation of ipsilateral whiskers.

RFs of barrel spiny stellate cells. An example of a recording from a spiny stellate cell the soma of which was located in the C2-barrel, close to the C3-barrel border, is shown in Fig. 1*A*–*C*. The cell's dendrites were asymmetric and were restricted to a single barrel (Figs 1*A* and 2). Deflection of both the PW (wC2, Fig. 1*B*) and a SuW (wD2, Fig. 1*C*) evoked large depolarisations, but APs only infrequently. The subthreshold RF structure of this cell (Fig. 2*A* and *B*) and that of another spiny stellate cell (Fig. 3*A* and *B*) comprised 5–8 whiskers. The dendritic arbors of these cells were asymmetric and confined to the PW-barrel borders. The cell illustrated in Fig. 2*C* and *D* had an axonal arbor with a few collaterals projecting to an adjacent barrel (also see the coronal view of the respective section, Fig. 2*D*). The cell illustrated in Fig. 3 also had an extensive axonal arbor that was, however, confined to lateral borders of the barrel-column.

The six spiny stellate cells shared morphological properties such as a strongly asymmetric dendritic arbor confined to barrel borders and spiny dendrites (Table 1). In five out of six spiny stellate cells axonal arbors were confined to barrel borders at the level of L4 but the analysis of axon morphology was compromised by the fact that not all axon branches were equally well stained. Barrel cells had a relatively high input resistance (Table 2). PW deflection evoked depolarising responses larger than 10 mV and depolarising responses predominated also in response to SuW whisker deflection. Cells had multi-whisker subthreshold RFs and the rate of evoked APs was low.

RFs of barrel pyramidal cells. Seven pyramidal cell somata were located within a barrel. Figures 4 and 5 show examples of the multi-whisker subthreshold RFs. Pyramidal cell somata were often located in the barrel centre in the upper part of L4, close to L3. Their dendritic arbor was confined to barrel-column borders and some

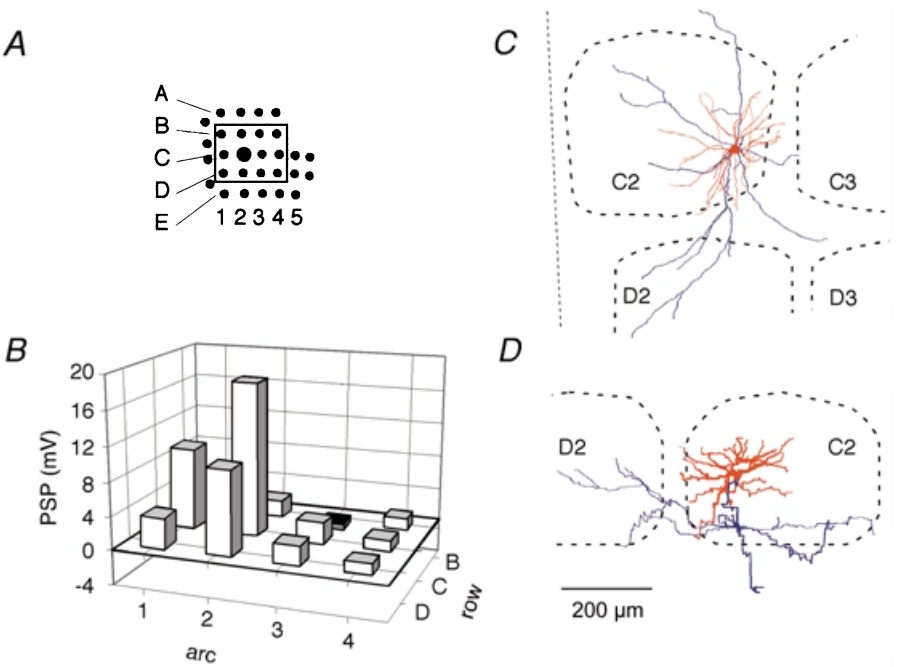

Figure 2. Subthreshold RF maps of a barrel spiny stellate cell

A, position of mapped whiskers. The box delineates those whiskers, whose responses were quantified. *B*, subthreshold peak response amplitude to onset of the deflection of different whiskers. Length of each bar represents amplitude of response. Position of the whisker is identified by the intersection of arc and row lines, respectively. *C*, dendritic and axonal arbors of the cell recorded from, when projected onto the horizontal plane, shown relative to barrel borders in the horizontal plane. *D*, same reconstruction projected onto a vertical plane, parallel to arc-2 (the projection plane is indicated in *C* by the dotted line).

Journal of Physiology

Table 1. Morphometric characteristics of L4 cells

	All cells $n = 23$	Barrel spiny stellate cells $n = 6$	Barrel pyramidal cells $n = 8$	Septum pyramidal cells $n = 5$
Cell type classification	6 spiny stellate 17 pyramids	6 spiny stellate	8 pyramids	5 pyramids
Soma diameter (μm)	17.3 ± 2.5	15.4 ± 2.3	18.3 ± 2.2	17.2 ± 2.9
Soma area (μm^2)	215 ± 68	172 ± 54	236 ± 67	223 ± 71
No. of dendrites	6.4 ± 1.8	6.3 ± 2.3	6.4 ± 1.7	7.4 ± 1.4
Total dendritic length (μm)	4934 ± 2741	2835 ± 901	4960 ± 2017	9420 ± 1798
Horizontal dendritic field span * (μm)	248 ± 44	215 ± 59	258 ± 56	267 ± 15
Vertical dendritic field span (μm)	623 ± 209	363 ± 105	741 ± 118	817 ± 130

No. of dendrites refers to primary dendrites; * measured along the arc of barrels.

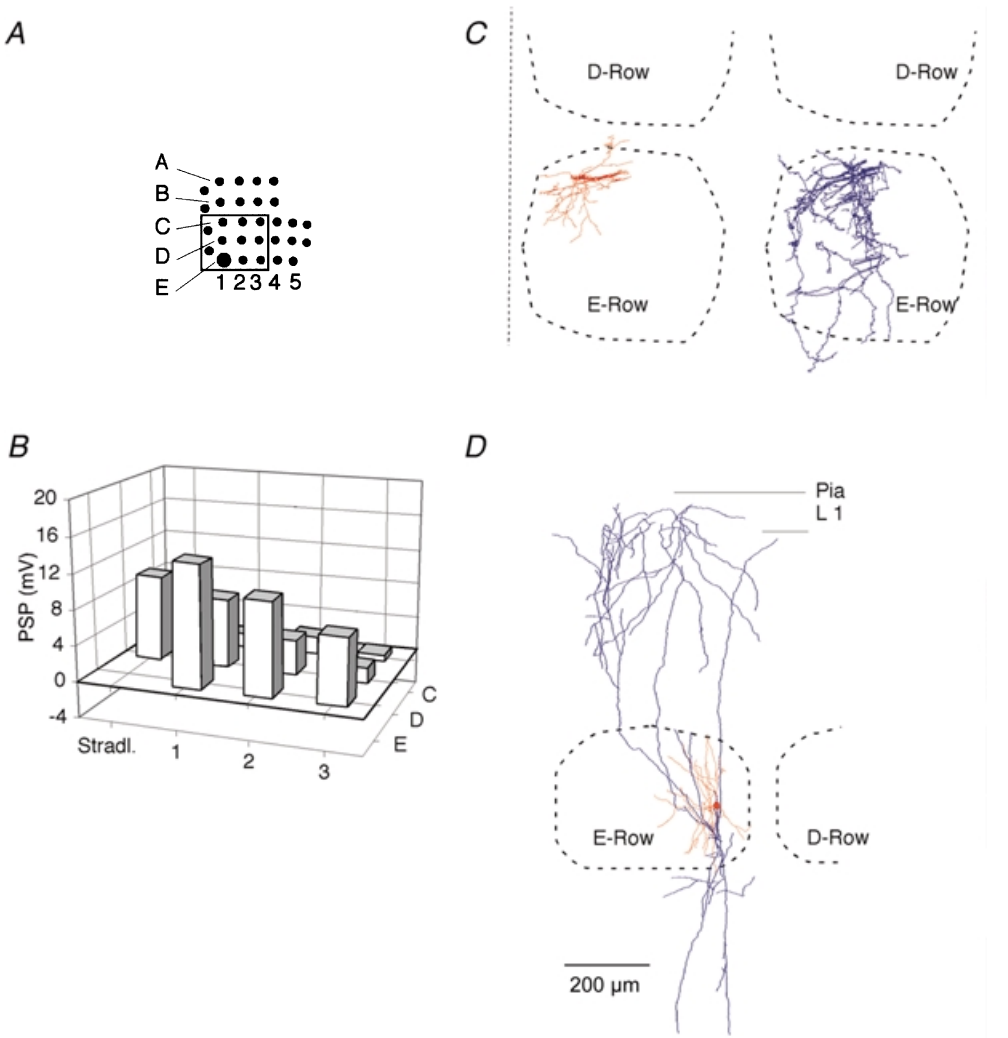

Figure 3. Subthreshold RF map of a barrel spiny stellate cell

A, position of mapped whiskers. *B*, subthreshold peak responses to deflection onset. *C*, left panel: dendritic arbor of the cell recorded from, when projected onto the horizontal plane, shown relative to barrel borders in the horizontal plane; right panel: axonal arbor of the cell recorded from, when projected onto the horizontal plane, shown relative to barrel borders. *D*, dendritic and axonal arbor projected to a vertical (coronal) plane shown relative to position of barrel borders (the projection plane used for *C* is indicated by the dotted line).

Table 2. Passive membrane properties of L4 cells

	All cells $n = 23$	Barrel spiny stellate cells $n = 6$	Barrel pyramidal cells $n = 8$	Septum pyramidal cells $n = 5$
RP (mV)	−81.8 ± 6.3	−81.5 ± 6.5	−82.9 ± 5.4	−78.8 ± 6.2
Steady state R_{in} (MΩ)	39 ± 19	53 ± 19	34 ± 19	23 ± 16
Depolarisation required for AP initiation (mV)	21 ± 5	19 ± 5	24 ± 5	21 ± 5

RP refers to the initial membrane resting potential; the value reported here refers to hyperpolarized membrane (down-) states. Steady state R_{in} refers to measurements made by injecting currents into the soma (hyperpolarising current of 100 pA), and determining the voltage change 300 ms after the beginning of current injection. AP thresholds were usually determined after several minutes of recording, i.e. under conditions where cells were 5–10 mV depolarised from their initial RP.

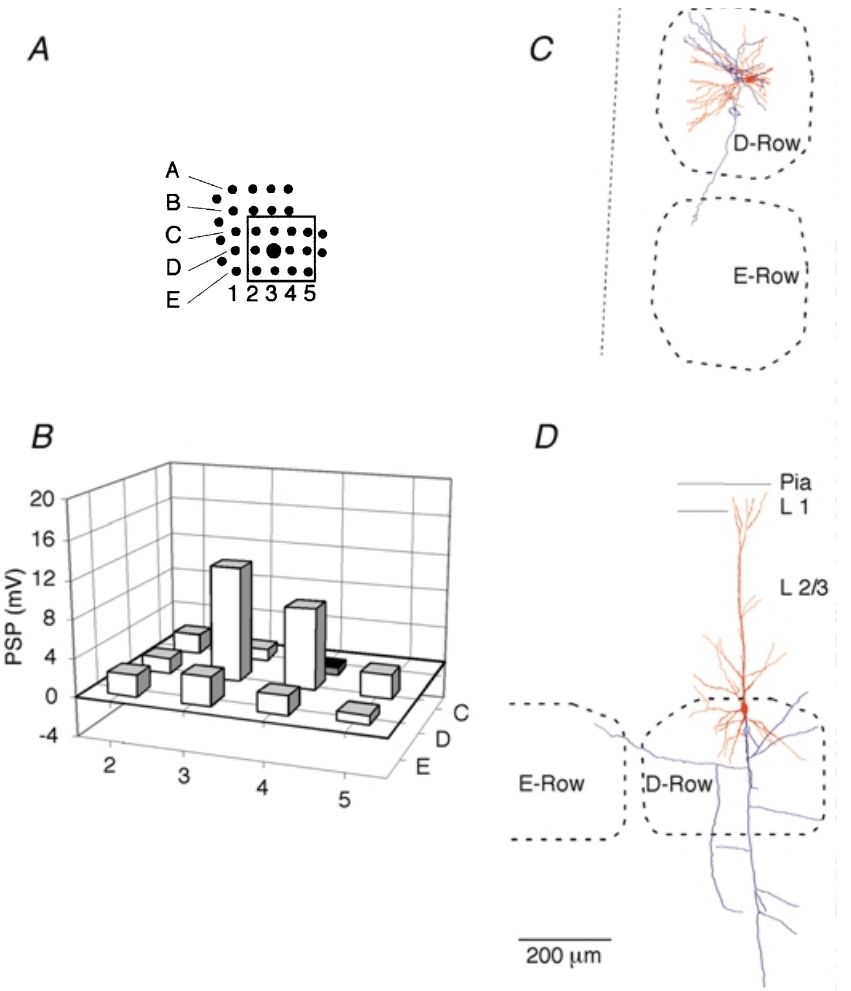

Figure 4. Subthreshold RF map of a barrel pyramidal cell

A, position of mapped whiskers. *B*, subthreshold peak responses to deflection onset. *C*, dendritic and axonal arbors of the cell recorded from, when projected onto the horizontal plane, shown relative to barrel borders in the horizontal plane. *D*, dendritic and axonal arbor projected to a vertical (coronal) plane shown relative to position of barrel borders (the projection plane used for *C* is indicated by the dotted line). The axon extends to the white matter, but reconstruction is not completely shown.

cells had an apical dendrite that terminated within L2/3 but was lacking an apical tuft. Thus these cells were identified previously as star pyramid cells (Lübke *et al.* 2000). Other pyramidal cells also had a tuft extending to the cortical surface (Table 1). The axonal arbors of five cells were confined to the borders of a barrel-column whereas two cells projected to adjacent columns.

The RF structure of barrel pyramidal cells was heterogeneous between cells. The majority responded with large depolarisation (>10 mV) to PW-deflection and their RF comprised between two and eight whiskers. The amplitudes of PW evoked PSPs of barrel pyramidal cells (11.4 ± 4.4 mV) were not significantly different from those of barrel spiny stellate cells (14.9 ± 4.5 mV) (Student's unpaired *t* test, $P > 0.05$).

RFs of septum pyramidal cells. Five pyramidal cells were located in a septum between barrels. Septum cells had between 6 and 10 primary dendrites and for each of the five cells the total dendritic length exceeded that of barrel cells (Table 1). Septum cells had significantly lower input resistances than barrel cells (unpaired *t* test, $P < 0.05$, Table 2), and their dendritic arbors were not confined to the borders of septa but extended partly into barrels. The axon collaterals of the cell shown in Fig. 6 projected selectively to other septa.

The PW responses were small compared to the responses evoked in barrel cells. One septum cell barely responded although the appropriate whiskers were stimulated. The cells had broad spatial tuning, i.e. only a small amplitude difference between PW and SuW responses. Responses of

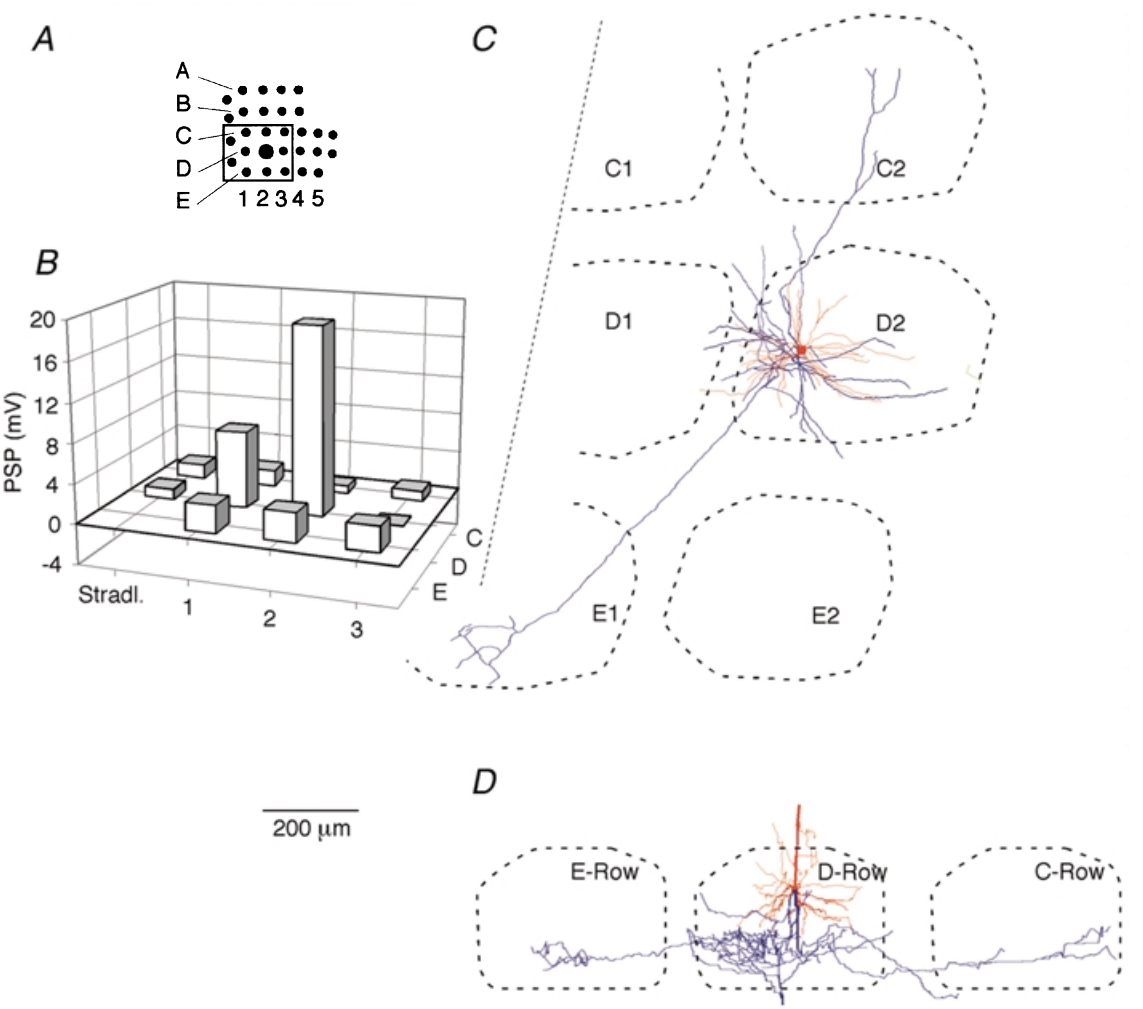

Figure 5. Subthreshold RF map of a barrel pyramidal cell

A, position of mapped whiskers. The box delineates those whiskers, whose responses were quantified. *B*, subthreshold peak response amplitude to onset of the deflection of different whiskers. Length of each bar represents amplitude of response. Position of the whisker is identified by the intersection of arc and row lines, respectively. *C*, dendritic and axonal arbors of the cell recorded from, when projected onto the horizontal plane, shown relative to barrel borders in the horizontal plane. *D*, same reconstruction projected onto a vertical plane, parallel to arc-2 (the projection plane is indicated in *C* by the dotted line).

septum cells to multi-whisker (airpuff) stimuli were substantially smaller (6.4 ± 2.7 mV) than the responses of barrel cells (12.6 ± 4.6 mV), but this difference did not reach significance (unpaired *t* test, $P > 0.05$).

Contribution of inhibitory inputs. Under our experimental conditions membrane potentials were close to the expected chloride reversal potential. As a consequence the contribution of inhibitory inputs to L4 cell PSPs was difficult to assess. We compared the time course and amplitude of PW responses in barrel neurons ($n = 7$) at their normal membrane potentials (in this sample around −75 mV, Table 2) with PW responses recorded while depolarising the same cells by current injection to a prestimulus membrane potential of −55 mV(data not shown). Inhibitory inputs should be hyperpolarising at this potential. The initial part of the responses (up to 9 ms poststimulus, when the response amplitude had attained about 40 % of its peak value) was almost unaffected by the predepolarisation. At 15 ms poststimulus time the amplitude of the response at the more positive potential was maximally reduced, by < 25 % (amplitude difference of 1.9 mV) compared to the responses evoked at resting membrane potential. At 25–30 ms after stimulus onset the responses recorded at depolarised membrane potential had similar or even larger amplitudes possibly indicating that a NMDAR-dependent conductance contributed to the PSP.

Dendritic and axonal arbor geometry and RF structure

Subthreshold RF structure was different for barrel and septum cells. A large (13.7 ± 4.6 mV) PW response and fewer SuWs characterise the average RF of barrel cells, whereas septum cells had a smaller PW response (5.7 ± 2.4 mV) and had a broader spatial tuning, i.e. comprised more SuWs. This difference in PSP response amplitude to PW stimulation was significant (unpaired *t* test, $P < 0.002$). Figures 7*A* and 8*A* show the average RF structure of barrel and septum cells respectively. Spiny stellate and pyramidal cells in barrels did not differ in RF structure and therefore the data were pooled.

The averaged barrel cell RF included all first order SuWs (Fig. 7*A*), meaning that cells in several barrels respond with depolarisation to deflection of a single whisker. On average the first order SuWs reached 30 ± 9 % of the PW response amplitude. In contrast, the average dendritic field span of barrel cells was confined to the borders of a single barrel (Table 3). Here 93 % of the total dendritic length were confined to the column of the home barrel (Fig. 7*B* and *D*). The difference between the multi-whisker RFs and

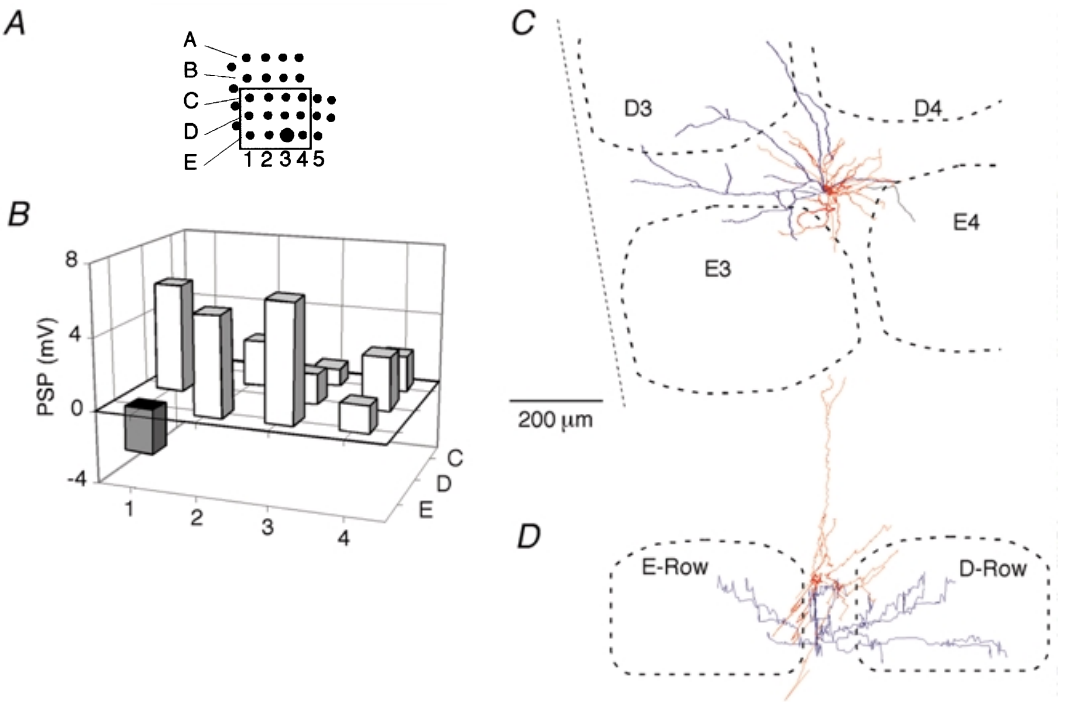

Figure 6. Subthreshold RF maps of a pyramidal a cell located in septum

A, position of mapped whiskers. The box delineates those whiskers, whose responses are illustrated. *B*, subthreshold peak response amplitude to onset of the deflection of different whiskers. Length of each bar represents amplitude of response. Position of the whisker is identified by the intersection of arc and row lines, respectively. *C*, dendritic and axonal arbors of the cell recorded from, when projected onto the horizontal plane, shown relative to barrel borders in the horizontal plane. *D*, same reconstruction projected onto a vertical plane, parallel to arc-2 (the projection plane is indicated in *C* by the dotted line).

confinement of the cell's dendritic arbor to a single barrel indicates that multi-whisker RFs are not a result of the dendritic field span of barrel cells. The axonal arbor field span (Fig. 7*C* and *E*) was restricted to the PW barrel-column in 7 of 10 identified barrel cells where 74 % of the total axonal length were confined to the column of the home barrel (Table 3). Thus, in L4 the intrabarrel axonal projections were 20-fold more dense than the axonal projection to a particular neighbouring barrel. The quantitative comparison of SuW response strength (black

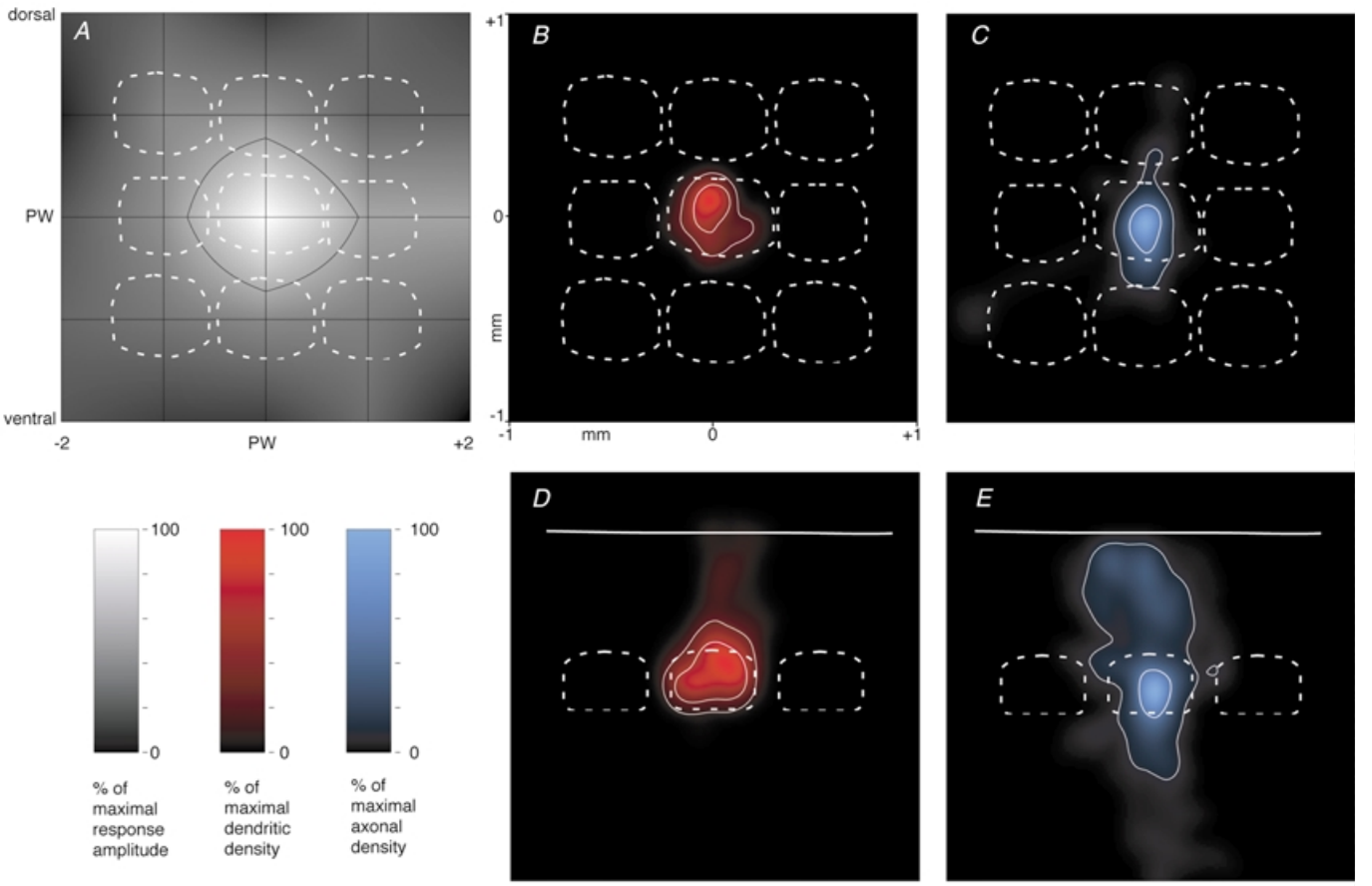

Figure 7. Comparison of averaged subthreshold RF map and dendritic and axon segment 2D density plots of barrel cells

A, average subthreshold RF map for barrel cells. The black grid indicates whisker positions, given with respect to the PW. Surround whisker positions are given by intersection of horizontal and vertical lines. The number −2 refers to SuW located in the second arc away from the PW in the caudal direction. The number +2 indicates whiskers in the second arc away from the PW in the rostral direction. The response amplitude is encoded by the brightness normalised to the peak of the PW deflection amplitude as determined in each individual experiment. The black contour line delineates an area on the RF map responding with ⩾ 50 % of the PW peak response amplitude. An average cytoarchitectonic barrel field pattern (white, dashed lines) in the horizontal plane is superimposed for comparison of the average RF structure of a barrel cell with the cytoarchitectonic barrel structure. Outlines above the PW barrel correspond to barrels located laterally of the PW barrel. Outlines right to the PW barrel outline correspond to barrels located anterior to the PW barrel. *B*, 2D map of dendritic 'length density' (red, $n = 6$) projected onto a horizontal plane. An average cytoarchitectonic barrel field projected into the horizontal plane (white, dashed lines) is superimposed for comparison with dendritic density map and barrel structure. Convention on location of barrels as in *A*. The inner white contour line delineates an area that contains densities that are ⩾ 50 % of the maximal density of dendrite segments. The outer white contour line delineates an area that includes 80 % of all dendritic segments. *C*, 2D map of axon 'length density' ($n = 6$, blue) projected onto a horizontal plane. Barrel field structure and white contour lines as described in *B* for dendritic segments. *D*, 2D map of dendritic length density ($n = 12$, red) projected onto a vertical plane. The map includes three spiny stellate cells whose barrel position was inferred from their asymmetric orientation of dendrites. The dashed lines represent outlines of averaged barrels. The outlines to the right of the PW barrel correspond to barrels located lateral to the PW barrel. White lines are contour lines as described in *B*. *E*, 2D map of axon length density ($n = 12$, blue). Projection onto a vertical, coronal plane along the arcs. Barrel outlines as in *D*, white lines are contour lines as described in *B*. Data from barrel cells include both spiny stellate and pyramidal neurons.

contour line in Fig. 7*A*) and dendritic and axonal densities (the central white contour lines in Fig. 7*B–E*) make it very unlikely that interbarrel connections can account for multi-barrel RFs of barrel cells, although they occur rarely in our material and could be more frequent (Fig. 5) with more complete axonal staining.

The average septum cell RF comprises more SuWs than the average barrel cell RF (Fig. 8*A*). The first order SuW responses reached 40 ± 16 % of the PW response amplitude. The dendritic arbor of the septum cells extended into adjacent barrels (Fig. 8*B* and *D*) and also the axonal arbor projected across the septum–barrel borders (Fig. 8*C* and *E*). The extent to which septum cell dendrites were confined to septa varied from cell to cell. In our sample only 64 % of septum cell dendritic length and 57 % of septum cell axonal length were confined to septum column as detailed Table 3. Thus the multi-whisker RFs of septum cells could, at least in part, result from their multi-barrel dendritic field spread.

Sub- and suprathreshold RF maps. Figure 9*A* and *C* shows suprathreshold RFs that were averaged across barrel and septum cells, respectively by aligning them with

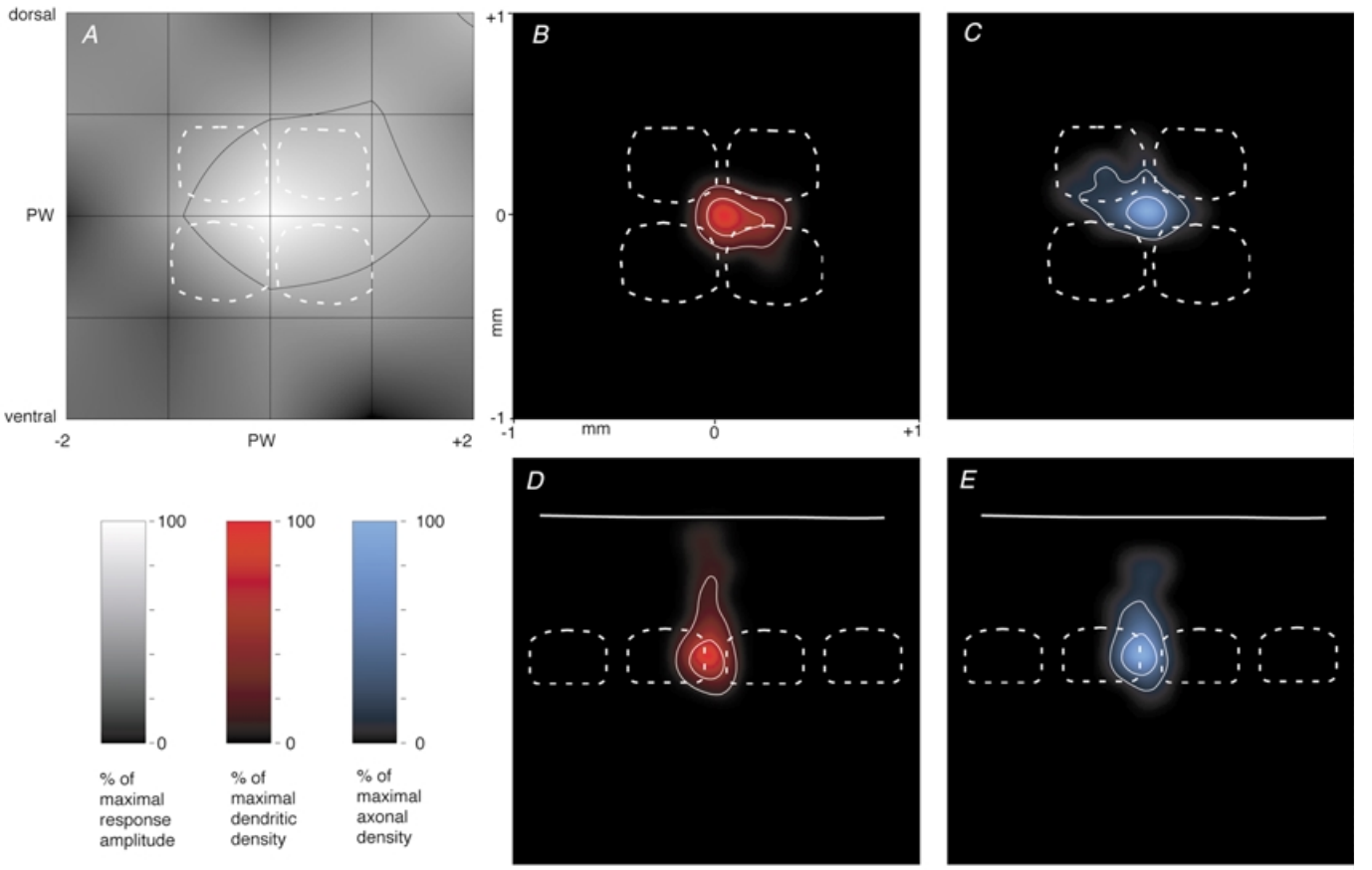

Figure 8. Comparison of averaged subthreshold RF maps and dendritic and axonal density plots of septum cells

A, average subthreshold RF map for septum cells. The black grid matches whisker positions given with respect to the PW as shown in Fig. 7. The central black contour line delineates the area responding to a response amplitude of 50 % or more of the PW deflection response. An average cytoarchitectonic barrel pattern in the tangential plane (white dashed lines) is superimposed for comparison of RF structure and cytoarchitectonic structure of the barrel field ($n = 5$ cells). Location of whiskers and barrels as described in Fig. 7*A*. *B*, 2D map of dendritic density (red, $n = 5$) projected onto a tangential plane. Cell reconstructions ($n = 5$) were aligned by superimposing the centres of their home septum prior to averaging. An average barrel pattern in the tangential plane (white dashed line) is superimposed for comparison between the dendrite density map and the dimensions of septa in the horizontal plane. The white contour lines delineate the areas that contain more than 50 % (inner line) of the maximal density of dendrite segments or more than 80 % of the total dendrite length (outer line). *C*, 2D map of axon length density (blue, $n = 5$) projected onto a horizontal plane. Barrel field structure and white contour lines as described in *B* for dendritic segments. *D*, 2D map of dendrite length density (red, $n = 2$), projected onto a vertical (coronal) plane along the arcs. The dashed lines represent outlines of averaged barrels, whereby outlines to the right from the septum correspond to barrels located laterally. White contour lines are as described in *B*. *E*, 2D map of axon length density (blue, $n = 2$), projected onto vertical (coronal) plane along the arcs. Barrel outlines as in *D*, white lines are contour lines as described in *B*.

Journal of Physiology

Table 3. Overlap of dendrites and axons of L4 cells with borders of barrel column in the shape of a cuboid

	Barrel cells		Septum cells *	
	Dendritic length	Axonal length	Dendritic length	Axonal length
Supragranular layers	96 %	85 %	64 %	60 %
L4	93 %	70 %	63 %	57 %
Infragranular layers	99 % **	71 %	80 % **	55 %

Percentage of dendrite or axon segments located within a barrel column or within a septum column. The cross section of mean barrel was 400 μm along the arc and 450 μm along the row. * Values represent only rough estimates, because they critically depend on the assessment of the barrel–septum border. ** Few dendrite segments were observed in these layers. Percentage of all dendritic and axonal segments located within a column defined as a vertical cylinder with the dimension of a barrel in the horizontal plane. The percentage values of septum cell dendrites and axons are given with respect to the dimensions of septa in the horizontal plane in layer 4.

respect to the subthreshold PW. Figure 9*B* and *D* illustrates the averaged subthreshold RFs for comparison. The spatial tuning of the suprathreshold barrel cell RFs was sharper than that of the subthreshold RFs. Septum cells only infrequently responded with APs.

Factors determining AP rate. Only 10 out of 23 cells responded with one or more APs to PW stimulation. To test whether the observed low AP rates were related to the dialysis of the cell during the whole-cell recording, we measured AP rates in the cell-attached recording

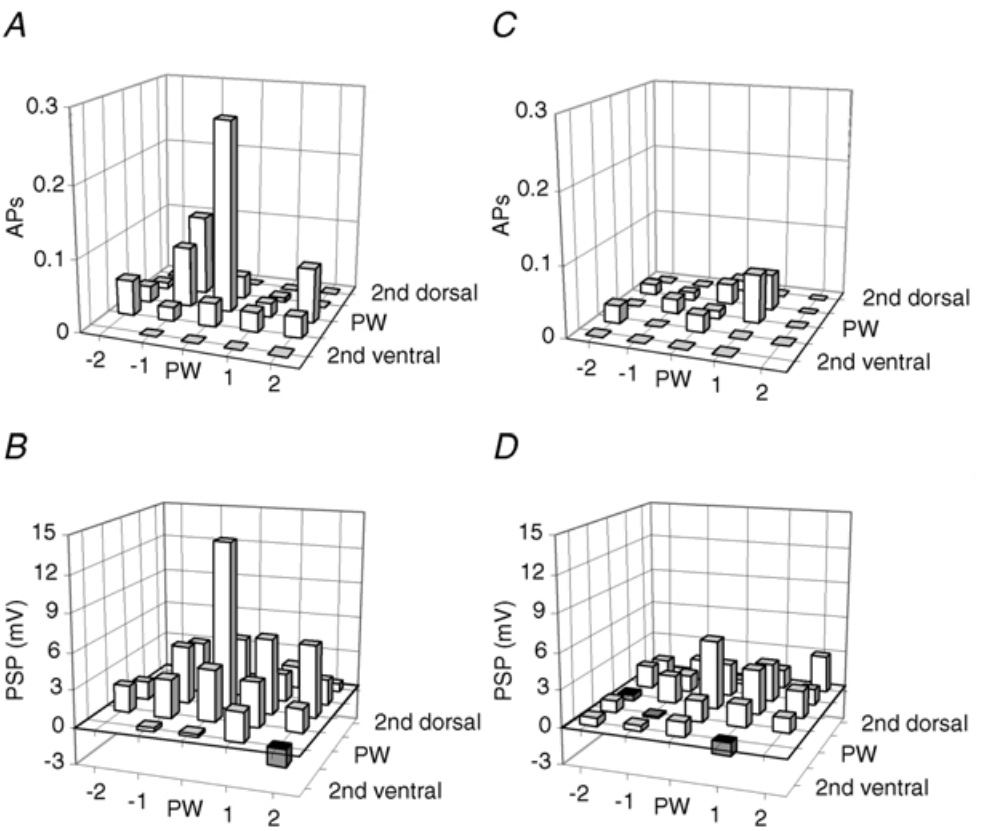

Figure 9. Comparison of averaged sub- and suprathreshold RF maps

A, average suprathreshold (AP) RF map for cells (n = 10) located in barrels. Prior to averaging RFs were aligned to the PW position determined by the subthreshold RF map. The position of a whisker is given by the intersection of horizontal and vertical lines. APs refers to number of APs per deflection. *B*, average subthreshold RF map for cells (n = 10) located in barrels. *C*, average suprathreshold (AP) RF map for cells (n = 5) located in septa. *D*, average subthreshold RF map for cells (n = 5) located in septa. To reveal the differential responsiveness of barrel and septum cells, the top two (*A* and *C*) and the bottom two graphs (*B* and *D*) have the same scale. *B*–*D*, conventions as in *A*.

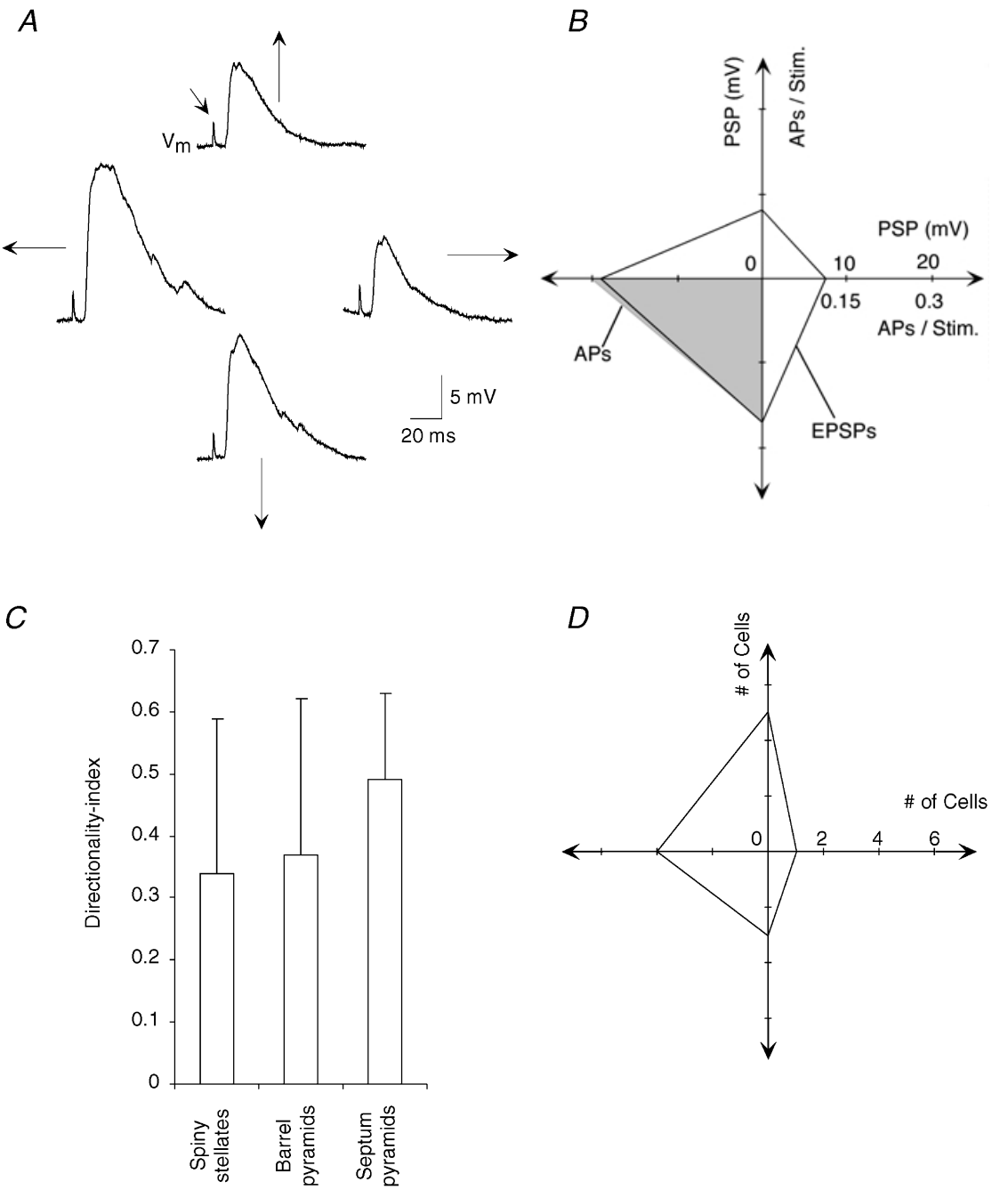

Figure 10. Direction sensitivity

A, subthreshold average responses of a barrel pyramidal cell to whisker deflection in different directions. Clockwise the direction is upward, forward, downward and backward as indicated by arrows. Stimulation artefacts are indicated by the small arrow in the top trace. Average responses from 20 stimuli. Calibration bars refer to all traces. *B*, direction tuning of PSPs and APs, same cell as shown in *A*. The four axes indicate (clockwise) upward, forward, downward and backward deflections. The shaded area refers to APs per stimulus. The lines indicate peak EPSP amplitudes. Same scaling for all directions as indicated for the forward direction. *C*, directionality indices for PSPs of different types of L4 cells tested ($n = 13$). A value of 1 would represent responses in only one direction whereas a value of close to 0 represents responses that are independent of direction of deflection. Error bars represent ± 1 S.D. Means are not statistically different. *D*, direction preferences of all recorded cells, convention for direction as in *B*.

configuration prior to whole-cell recording (Margrie *et al.* 2002). Spontaneous AP rates were consistently lower before whole cell break-in than after, indicating that loading increased rather than decreased the AP activity (data not shown). AP rates could be low because the cell's membrane potential was well (15–35 mV) below AP threshold (Table 2). This view is supported by current injection experiments because *I–V* plots indicated that an average depolarisation of 21 ± 5 mV was required for evoking APs ($n = 23$). Similarly analysis of the relationship between evoked PSP amplitudes and AP rates showed that a PSP amplitude larger than 20 mV was required to reliably (>50 % of stimuli) elicit APs.

Functional differences between stellate and pyramidal cells in barrels

The two classes of barrel cells differ in some of their functional properties and these differences might be related to the different geometry of their dendritic arbors.

Direction sensitivity. The responses of L4 neurons to stimuli of four different directions were studied in a subset of cells ($n = 13$). An example of direction dependent responses is shown in Fig. 10*A* and *B*. The AP responses were more direction selective than subthreshold depolarisations both in the example shown in Fig. 10*B* and at the population level (data not shown). The three septum cells tested were more direction selective than most barrel cells, suggesting a further difference between barrel and septum cells (Fig. 10*C*). The directionality of responses of barrel spiny stellate and pyramidal cells was similar. The overall distribution of preferred directions was biased towards upward and backward deflections (Fig. 10*D*).

Multi-whisker *vs.* single-whisker stimulation. The relative response strength of stellate and pyramidal cells to a single PW deflection and to an optimally positioned multi-whisker airpuff was different. While spiny stellate cells responded preferentially to the PW stimulus both barrel and septum pyramidal cell responded preferentially to multi-whisker deflection (Fig. 11, left and right panels). In stellate cells the response to an airpuff stimulus was only 50 ± 51 % of a PW response, whereas in pyramidal cells it was 120 ± 49 %. The difference between stellate and pyramidal cells in the ratio of PW response and airpuff response was significant (unpaired *t* test, $P < 0.01$).

Temporal properties of barrel and septum cell responses

In the previous section we measured the peak depolarisation to construct RFs for different cell types. However, the deflection evoked depolarisations were characterised by a time course that was different between barrel and septum cells and moreover they depended on the position of the stimulated SuW with respect to the PW. Thus the spatial extent of the representation of a whisker deflection in L4 cells is time dependent.

Time course of PW responses. The left panels in Fig. 12*A–C* show 10 superimposed traces of PW responses recorded in the three different classes of L4 cells. The spiny stellate cell (Fig. 12*A*) and the pyramidal cell (Fig. 12*B*) had large amplitude, fast rising responses. In the few barrel cells, which discharged at relatively high rates, APs occurred with short latency and were tightly locked to stimulus onset. In comparison the responses in the septum cell rose more slowly (Fig. 12*C*).

The AP rates in L4 evoked by PW stimulation differed widely between different cells (Fig. 12*A–C*, right panels). The overall AP rate was low, 0.14 ± 0.29 APs per PW stimulus and only barrel cells contributed substantially to the response histogram (Fig. 12*D*). The AP responses of barrel cells' deflection were maximal at 11–14 ms for deflection onset (Fig. 12*D*). Seventy-six per cent of APs evoked by PW stimulation occurred as single AP

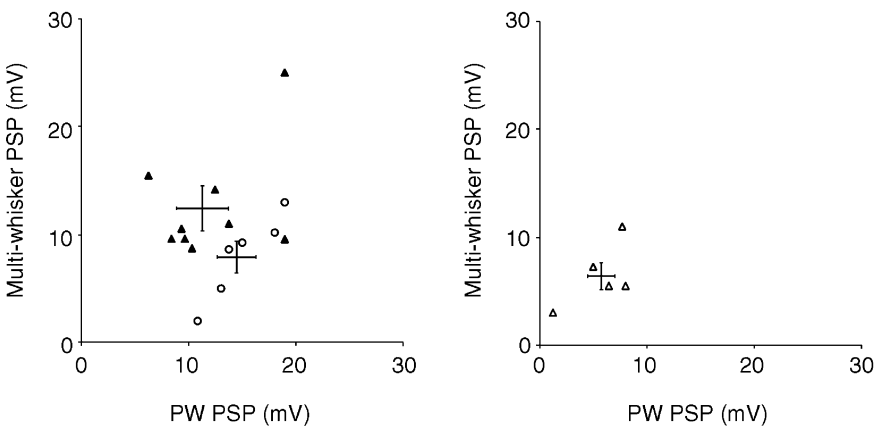

Figure 11. Single- and multi-whisker stimulus responses

Plots of multi-whisker stimulus depolarisation amplitudes against single-whisker PW deflection depolarisation amplitudes in barrel cells (left) and septum cells (right). Symbols represent spiny stellate cell (open circles), barrel pyramidal cells (filled triangles), septum pyramidal cells (open triangles). Crosses indicate means ± S.E.M.

responses, 19 % of APs occurred in doublets and 5 % of APs occurred as triplets; the criterion for counting APs as part of a doublet or triplet was a separation of less than 20 ms between APs. Responses to deflection onset were larger (153 % for PSPs) than those to deflection offset and this difference was significant (paired Student's t test, $P > 0.001$). To further quantify this observation we defined an On/Off index as: (OnPSP − OffPSP)/(OnPSP + OffPSP). This index, which becomes 1 for purely On responsive cells and −1 for Off responsive cells, was 0.11 ± 0.20 across all L4 cells.

The averaged response time course of spiny stellate cells and pyramidal cells in barrels was similar. In particular, the 20–80 % amplitude rise time of spiny stellate PSPs

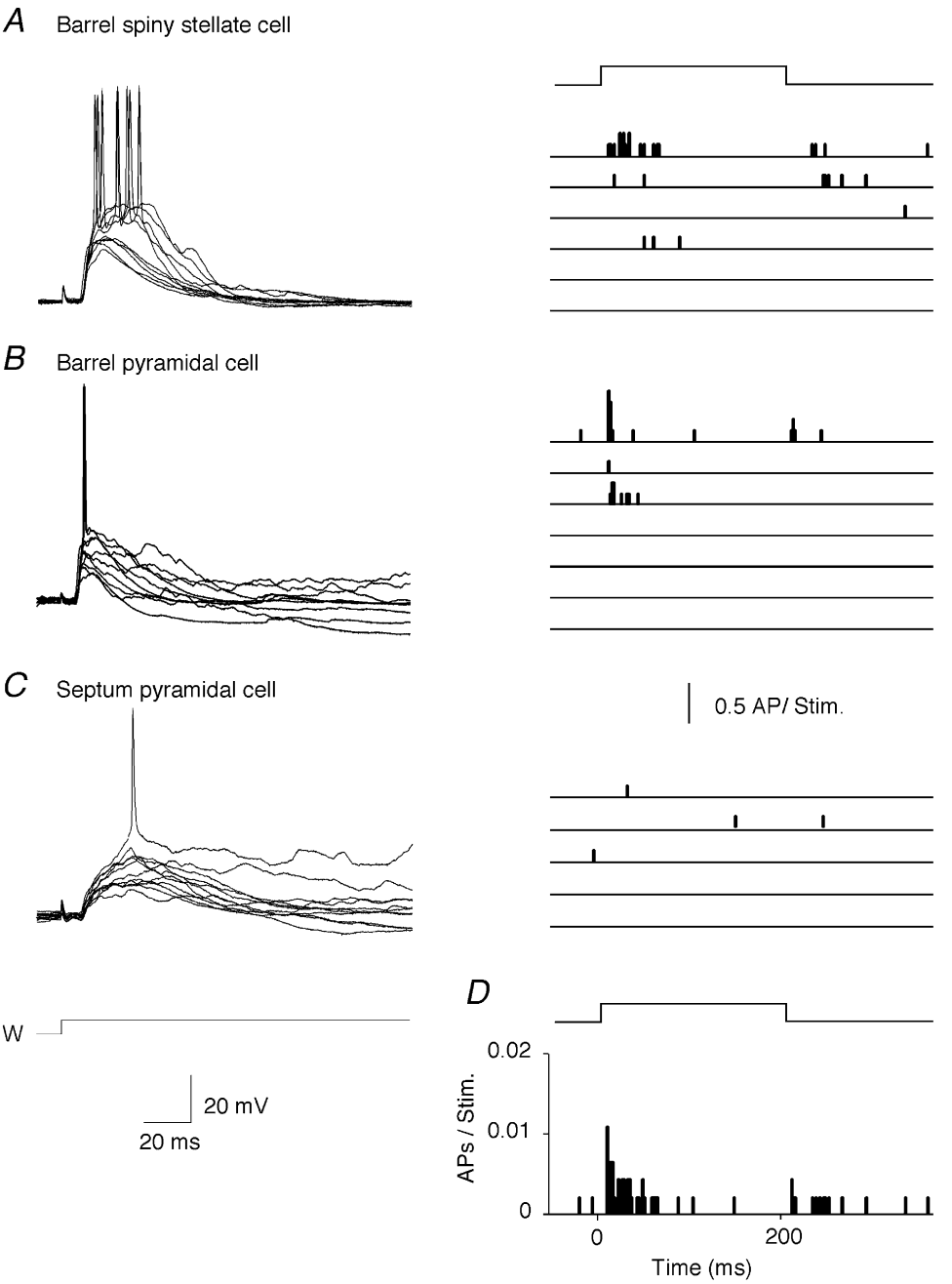

Figure 12. AP responses of barrel and septum cells

A, left: records of 10 superimposed responses of a spiny cell to PW deflection; right: peri-stimulus time histograms (PSTHs) of six spiny stellate cells. *B*, left: ten superimposed responses to PW deflection of a barrel pyramidal cell, right: PSTHs of seven barrel pyramidal cells. Four cells did not respond with APs. *C*, left: ten superimposed responses to PW deflection of a septum pyramidal cell; right: PSTHs of five septum cells, two cells did not respond. *D*, population PSTH of all L4 cells. AP responses of five pyramidal cells of undetermined position within a barrel have also been included. Bin width of PSTHs is 0.5 ms. The peak AP response to stimulus onset is at 11.5 ms.

(3.1 ± 1.8 ms) and of barrel pyramidal cell PSPs (2.7 ± 1.5 ms) were not significantly different (unpaired *t* test, $P > 0.05$). In contrast, the 20–80 % amplitude rise time of barrel cell PSPs (2.8 ± 1.8 ms) and of septum cell PSPs (6.1 ± 2.5 ms) were significantly different (unpaired *t* test, $P < 0.05$). Also the peak latency (15.0 ms) and the decay time constant (60 ms) of the averaged barrel cell response were shorter than the average septum cell response (peak latency 22.3 ms and decay time constant was 85 ms).

Whisker position and response time course. Figure 13*A* and *B* shows traces of responses to stimulation of different whiskers in the RF of a spiny stellate and a septum pyramidal cell, respectively. While response latencies of barrel spiny stellate and barrel pyramidal cells were similar (data not shown), latencies of barrel (onset latency 8 ± 1.4 ms) and septum cells(onset latency 11 ± 2.0 ms) were significantly different (Fig. 13*C*, *D*). The onset latency increases with distance of the SuW from the PW and was shorter for the barrel cell than that of the septum cell (Fig. 13*A*–*D*). The time course of whisker responses in a particular cell may be indicative of the source of input that drives the responses. Thalamic APs are evoked during a narrow time window and have a short latency (Waite,

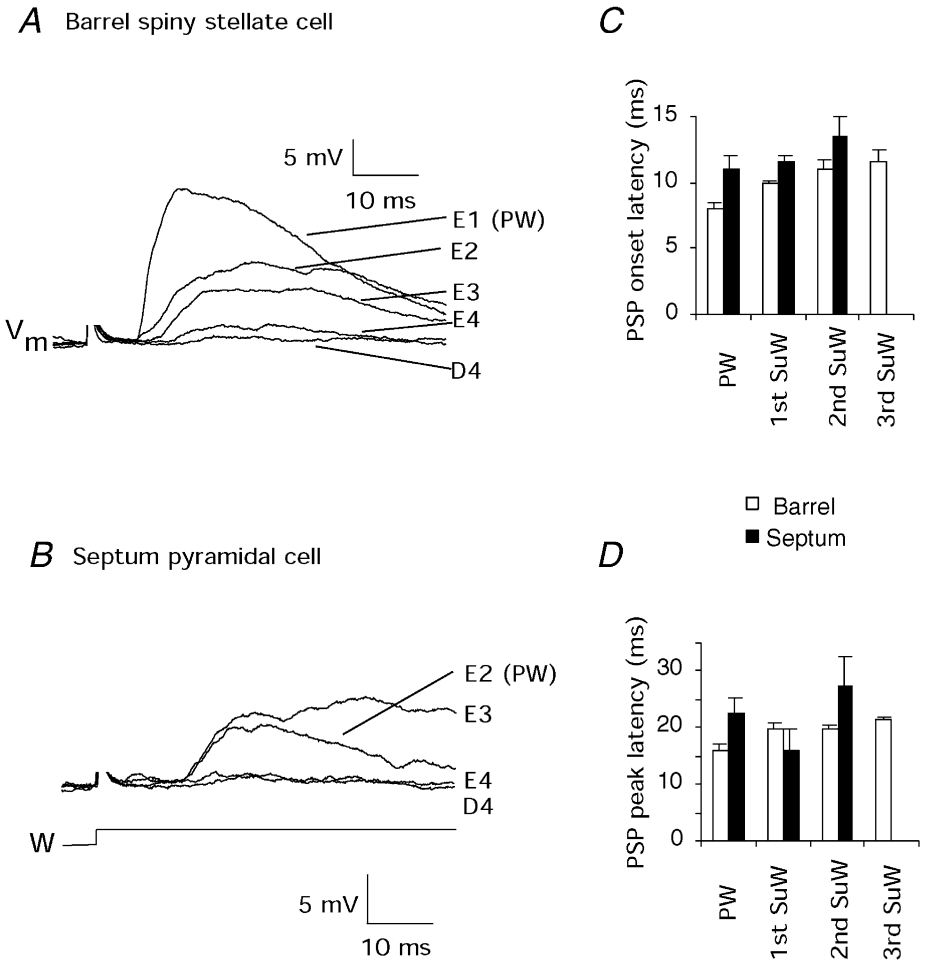

Figure 13. Response latency in barrel and septum cells

A, response onset latencies in a barrel cell in response to deflection of whiskers at different RF positions. The labels on each trace refer to the whisker deflected. E1 is the PW. Records with median latencies are selected for each whisker position. *B*, response onset latencies in a barrel cell deflections of whiskers at different RF positions Stimulus artefacts are partially blanked in *A* and *B*. Calibration in *A* applies to *A* and *B*. *C*, population statistics for response onset latencies of barrel (open bars) and septum (filled bars) cells, error bars indicate ± 1 S.E.M. Mean (± 1 S.D.) onset latencies for barrel and septum cells are respectively: PW 8.0 ± 1.4 ms and 11 ± 2 ms, 1st order SuW 9.9 ± 2.1 ms and 11.6 ± 2 ms, 2nd order SuW 11.0 ± 4.2 ms and 13.5 ± 2.8 ms. The differences between barrel and septum cell onset latencies are significant for all whisker positions. *D*, population statistics for response peak latencies of barrel (open bars) and septum (filled bars) cells, error bars indicate ± 1 S.E.M. Mean (± 1 S.D.) peak latencies are for barrel and septum cells, respectively: PW 15.0 ± 6.8 ms and 22.3 ± 6.8 ms, 1st order SuW 19.6 ± 6.8 ms and 15.8 ± 8.6 ms, 2nd order SuW 19.9 ± 5.8 ms and 27.4 ± 8.9 ms. The differences between barrel and septum cell onset latencies are significant for PW and 2nd order SuW responses.

1973; Ito, 1988; Simons & Carvell, 1989; Diamond, 1995; Brecht & Sakmann 2002), whereas cortical responses occur with a substantial delay and relatively large temporal scatter (Armstrong-James, 1995; Brecht & Sakmann, 2000; Pinto *et al.* 2000). Large amplitude depolarisation, with short onset latency and short peak latency may reflect a dominant VPM contribution whereas the long onset and delayed peak responses may indicate a dominant contribution from intracortical connections. We found that in all but one barrel cell the PW responses shared characteristics, such as a large PSP amplitude and short onset and peak latencies consistent with a strong thalamic contribution to these responses. Most SuW responses had longer onset and peak latencies (Fig. 13*C*, *D*). All large SuW responses (> 10 mV) had short onset and short peak latencies, suggesting that thalamocortical excitation is a primary source of these responses.

Time dependence of RF structure. The RF structure changed as a function of time after stimulus onset depending on the cell type. To assess this dynamic change quantitatively we measured response amplitudes for different time points after a whisker deflection. The results (Fig. 14) indicate that barrel cell responses emerged at 10 ms as a single-whisker RF, and then the RF expanded rapidly, within 15 ms after stimulus onset, to their maximal size and peak amplitude at 15 ms (Fig. 14, upper panel). Barrel cell responses had vanished at about 80 ms after stimulus onset. Septum cell responses usually emerged as multi-whisker RFs and expanded in size and amplitude up to 40–60 ms (Fig. 14, lower panel). Septum responses vanished only after more than 150 ms.

Short-term modification of responses during repetitive PW deflections. Rodents often engage their vibrissae in rhythmic whisker movements at frequencies between 5–15 Hz (Welker, 1964; Carvell & Simons, 1990). In response to 10 Hz trains of PW deflections the three spiny stellate cells tested show facilitating or maintained, non-depressing responses (Fig. 15*A*) as the tenth response was > 100 % of the first response in the train. In contrast in all barrel pyramidal ($n = 7$, Fig. 15*B*) and septum pyramidal cells ($n = 4$, Fig. 15*C*) the response amplitude decreased as the tenth response was < 65 % of the first response in the train, with septum cells showing the strongest depression (Fig. 15*C*).

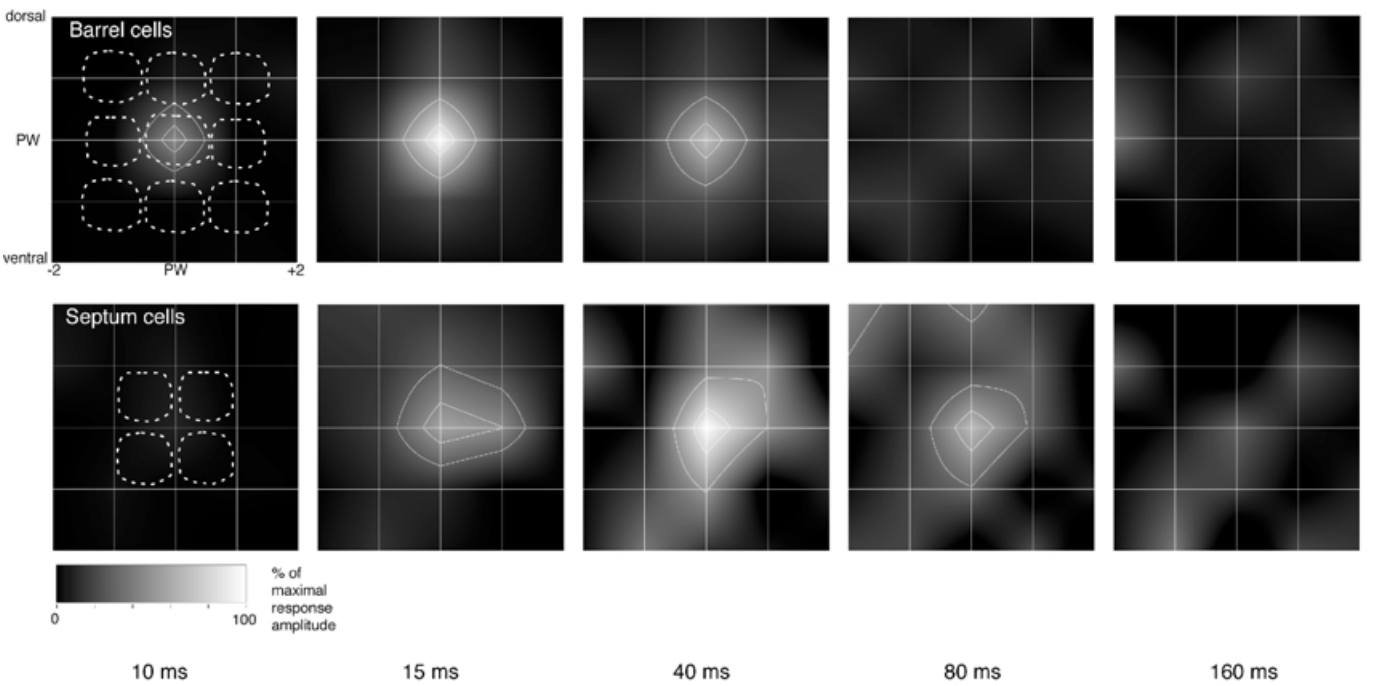

Figure 14. Time dependence of subthreshold RF structure of barrel and septum cells

The grid of white lines represents the localisation of a whisker with respect to the PW as intersection between horizontal and vertical lines. Response amplitudes are normalised with respect to the response to PW stimulation. Top, averaged and smoothed subthreshold RFs of barrel cells ($n = 5$ cells) at different times after whisker deflection. The same grey scaling applies to all RF plots. The white lines delineate the area of ⩾ 80 % and ⩾ 50 % of the maximal response to PW stimulation (maximal response at 15–20 ms for barrel cells and at 40 ms for septum cells). For clarity, the contour lines are shown only in those RF plots where the response reaches at least 50 % of the maximal amplitude. The dashed white lines delineate the outlines of average anatomical barrels arranged around the PW barrel. Barrel identification as in Figs 7 and 8. Bottom, same plots for four septum cells. Same conventions as in Figs 7*A* and 8*A*.

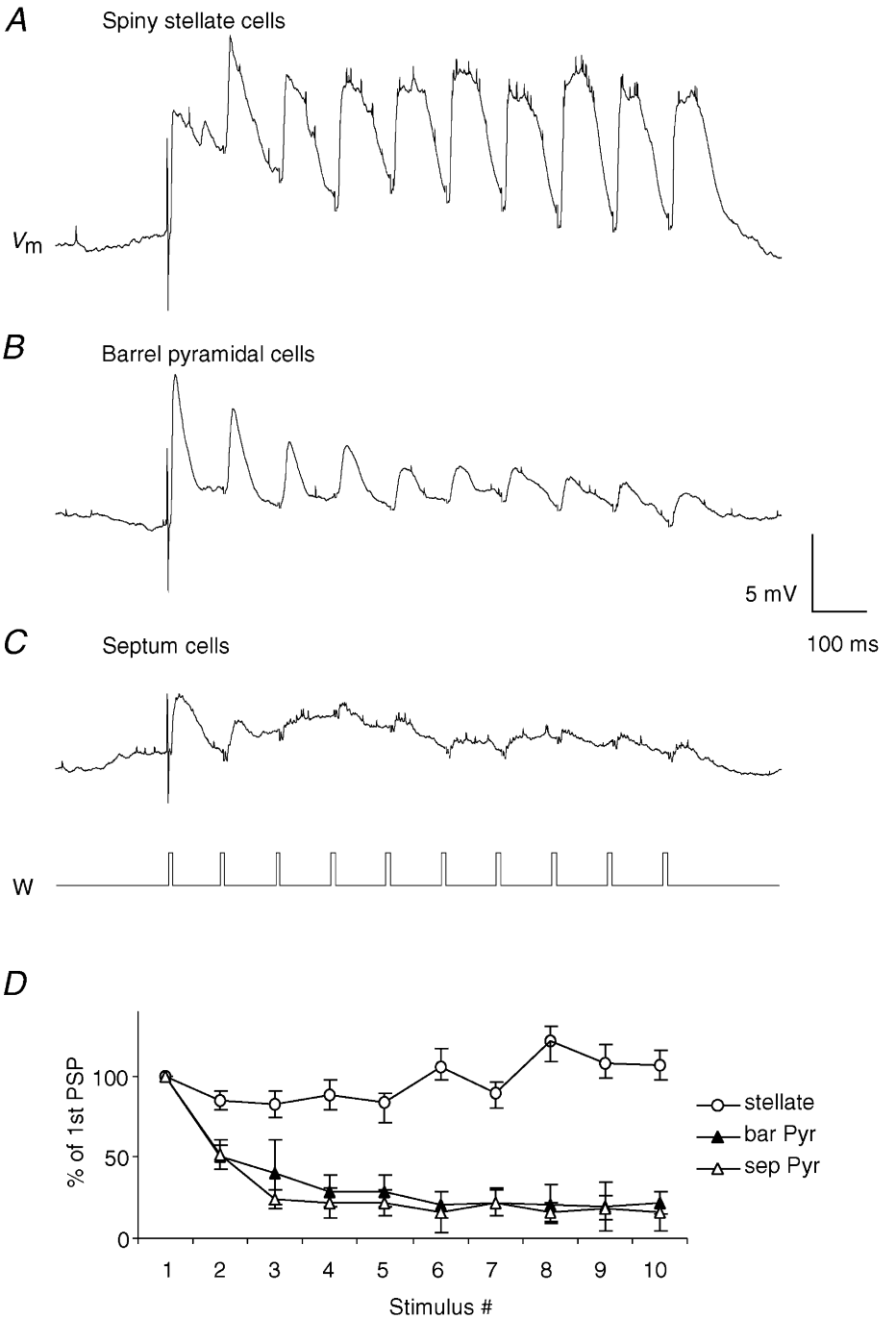

Figure 15. Responses of barrel and septum cells to repetitive PW stimuli

Stimuli were brief (2 ms) backward and forward deflections (6 deg) in the horizontal direction applied at 10 Hz. All but the first needlelike stimulation artefacts in the respective traces (V_m) have been blanked. Bottom trace labelled 'w' indicates sequence of whisker deflections. *A*, response average of three spiny stellate cells. Peak response amplitudes to each deflection in the train is maintained. *B*, response average of eight barrel pyramidal cells with decreasing peak response amplitude during the train. *C*, response average of four septum pyramidal cells with strongly decreasing peak response amplitude. *D*, dependence of PW evoked subthreshold peak responses normalised to the response evoked by the first deflection in a train. Spiny stellate cell (open circles) maintain their response, barrel pyramidal cells (filled triangles) and septum pyramidal cells (open triangles) show smaller responses with successive deflections in the train.

DISCUSSION

Main findings

The amplitude and time course of responses to whisker deflections in identified L4 cells indicate that these neurons have multi-whisker RFs, comprising a PW and several SuWs, comparable to RFs of non-identified neurons in L4 (Moore & Nelson, 1998; Zhu & Connors, 1999). Thus a barrel or a septum comprises an ensemble of a few thousand neurons, each of which is driven predominantly by the same PW together with weaker inputs from SuWs, which however vary in number for each particular neuron. According to our results structure–function relationships in the cortical network become apparent only when the vertical position (layer), and the horizontal position (barrel *vs.* septum) are evaluated in combination with a cell's dendritic and axonal arbor. The present work suggests that three anatomically defined classes of neurons in L4, i.e. the spiny stellate and star pyramidal cells as characterised functionally and anatomically in acute slices (Feldmeyer *et al.* 1999; Lübke *et al.* 2000) and the pyramidal cells in septa vary in the way they represent the spatial and temporal properties of tactile stimuli. This finding raises several questions. Firstly, how do the sub- and suprathreshold depolarisations that define the RF depend on the extent and location of the cell's dendrites and how do their RFs reflect the thalamocortical connections. Secondly, how are variables of whisker stimuli like the number, amplitude and temporal sequence of deflected whiskers represented in each class of cell. Finally, how may the properties of the animal's tactile environment be represented in L4 by sub- and suprathreshold potentials in specific ensembles of neurons in barrels and septa respectively.

Functional properties of three morphological classes of neurons in layer 4

Barrel and septum cells. The responses of cells located in barrels were very different from those of the septum cells. Barrel cells have shorter depolarisation onset latencies and larger peak depolarisation than septum cells, consistent with the differences in origin and pattern of thalamic innervation of barrels and septa (for review see Kim & Ebner, 1999). For both barrel and septum cells the RF structure is time dependent; however the RF structure in septum cells develops later and comprises more SuW barrels and the responses decay more slowly after stimulus termination. These functional differences between barrel and septum cells reflect separate afferent inputs from the thalamus. While barrel cells receive fast focal input from the VPM nucleus (Diamond, 1995), septa receive afferent input from axons originating in the posterior medial (PoM) nucleus (Koralek *et al.* 1988; Chmielowska *et al.* 1989) and these axonal arbors project over relatively long distances within septa (Lu & Lin, 1993). Similar to septum cell responses described here the PoM cell unitary responses also have relatively long latencies, a broad spatial tuning and a relatively small peak response amplitude when evoked by single whisker deflection (Diamond *et al.* 1992; Diamond, 1995).

Barrel stellate and barrel pyramidal cells. Spiny stellate cells respond with depolarisations that are maintained during repetitive (10 Hz) whisker deflections whereas the pyramidal cells' responses depress. The sustained nature of spiny stellate responses is comparable to sustained AP responses of thalamic VPM cells (Hartings & Simons, 1998). Assuming that both classes of cells are innervated by the same class of VPM cells this could indicate that the release properties of VPM cell terminals are target cell specific as reported in other cortical connections (Reyes *et al.* 1998, Rozov *et al.* 2001). In addition, the response amplitude of spiny stellate cells decreases with the number of whiskers deflected resembling also the response pattern of VPM cells, which respond less to multi-whisker stimuli compared to single-whisker stimulation (Brecht & Sakmann, 2002).

Dendritic arbors and thalamocortical circuitry

The dendritic arborisation of the cells located in barrels is qualitatively similar to that described previously (Woolsey *et al.* 1975; Simons & Woolsey, 1984; Lübke *et al.* 2000; Petersen & Sakmann, 2001). The larger number of pyramidal cells recorded from, relative to spiny stellate cells, could reflect a sampling bias of whole-cell recording with patch pipettes for large somata. Alternatively, the high incidence of pyramidal cell recordings may also be related to the fact that our recordings were targeted to the postero-medial barrel subfield (PMBSF), where a larger number of pyramidal neurons is observed (Elston *et al.* 1997) and that most of our cells were located in the upper part of L4, with a proportionally higher percentage of pyramidal cells (Simons & Woolsey, 1984).

The dendritic fields of spiny stellate and pyramidal cells were confined to a single PW barrel-column (Table 3; Simons & Woolsey, 1984; Lübke *et al.* 2000; Petersen & Sakmann, 2001). However all cells had multi-whisker subthreshold RFs. Thus the question arises as to the anatomical connections that mediate the multi-whisker RFs. The short onset and peak latency as well as the large amplitude of PW-evoked depolarisations in barrel cells suggest that axon terminals of thalamic single whisker excitation (SWE) cells in the VPM are the major afferents (Simons & Carvell, 1989; Armstrong-James *et al.* 1991; Brecht & Sakmann, 2002). SuW responses with large amplitude (> 10 mV) were comparable to PW responses with respect to onset and peak latencies. Thus SuW responses are likely to be generated, to a larger extent, by divergent thalamic SWE cell inputs. The fact that large amplitude SuW responses were of short latency is consistent with the conclusions of Goldreich *et al.* (1999),

who suggested a thalamic origin of suprathreshold (AP) responses to SuW stimulation but is at variance with the conclusions of Armstrong-James *et al.* (1991). The view of thalamocortical divergence suggested by RF structure and dendritic arborisation is supported by direct anatomical evidence showing divergent axon projections of thalamic VPM to multiple, adjacent barrels (Arnold *et al.* 2001) and by the observation that the interbarrel projections are sparse (Fig. 7 and Table 3) (see also Lübke *et al.* 2000; Petersen & Sakmann, 2000, 2001).

The SuW responses with small amplitude (< 10 mV), because of their longer onset and peak depolarisation latencies could be generated by inputs from thalamic afferents of multi-whisker excitation (MWE) cells in the VPM (Brecht & Sakmann, 2002) which have a longer response latency or by the sparse interbarrel connections in L4 (V. Egger and B. S., unpublished observations). Barrel pyramidal cells have, in addition to their basal dendrites, a prominent apical dendrite and we suggest that additional thalamic or cortical inputs to the apical dendrites may account for their stronger activation by multi-whisker stimuli.

Whisker responses in L4 cells reflect presumably composite EPSPs and IPSPs but deflection evoked inhibition in L4 cells is transient and maximal at the response peak, comparable to observations in supra- and infragranular cells of barrel cortex (Moore & Nelson, 1998; Zhu & Connors, 1999) and in morphologically unidentified cells of visual cortex (Borg-Graham *et al.* 1998). In L4 cells the contribution of inhibition to evoked PSPs seems to be comparatively weak, consistent with the smaller effects in L4 of bicuculline on columnar voltage sensitive dye (VSD) responses (Petersen & Sakmann, 2001). Inhibition in L4 cells of barrel cortex is also substantially weaker than in thalamic VPM cells (Brecht & Sakmann, 2002). In VPM cells excitatory and inhibitory components are temporally dispersed and appear as a sequence of predominant depolarisation followed by predominant hyperpolarisation. Both components are also spatially segregated into predominantly excitatory and inhibitory whisker projections (Brecht & Sakmann, 2002).

Representation of whisker deflections in barrels by sub- and suprathreshold depolarisation

A large difference between whole-cell voltage and extracellular unit recordings are the low rates of spontaneous (0.053 APs s^{-1}) and evoked (0.14 APs per PW stimulus) AP activity. With few exceptions (Dykes & Lamour, 1988) unit recording studies, which employed the same anaesthesia as we did, report spontaneous AP rates between 0.8 and 1.54 APs s^{-1} (Armstrong-James *et al.* 1994; Huang *et al.* 1998), and evoked AP rates between 1 and 1.4 APs per PW stimulus (Armstrong-James & Fox, 1987; Armstrong-James *et al.* 1992; Diamond *et al.* 1993). Since urethane anaesthesia is thought to be associated with an increased excitability (Simons *et al.* 1992), and studies using other or no anaesthesia also reported higher evoked AP rates (Simons, 1978, 1985; Simons & Carvell, 1989), we infer that the low AP rates do not result from urethane anaesthesia. Cell-attached current recordings from barrel cells indicate that low AP rates did also not result from loading cells with the pipette solution (Margrie *et al.* 2002). It seems likely that extracellular unit recording and whole-cell recording *per se* may lead to different estimates of AP activity in the cortex. One possible cause is a sampling bias of unit recordings against non-spiking cells (see Moore & Nelson, 1999; Zhu & Connors, 1999).

Massive or sparse and selective synaptic input and computation of output in L4. How do sub- and suprathreshold RFs reflect the synaptic input to individual cell types in L4? The average peak PSP evoked by a PW deflection in a barrel neuron was about 14 mV whereas the size of unitary EPSPs, in connections between barrel neurons *in vitro* is 1.6 mV. A barrel cell receives about 160 unitary inputs in addition to thalamocortical and other, intracortical inputs (Feldmeyer *et al.* 1999). Thus, taking into account a temporal scatter of barrel cell APs, as few as 10–15 unitary inputs (representing about 10 % of a cell's inputs from other L4 cells and probably less than 5 % of its total synaptic inputs) could generate the depolarisation evoked by a PW-whisker deflection. Assuming in addition that AP rates in response to PW stimulation are, on average, as high as reported in unit recordings (AP rates $\geqslant$ 1 AP per PW stimulus per cell), it follows that more than 95 % of the subthreshold excitatory L4 inputs should be balanced by concomitant inhibitory input. Massive, excitatory and inhibitory inputs that balance each other and generate only a moderate net depolarisation have been referred to as a 'high input'-computation regime (Shadlen & Newsome, 1998; see also Bernander, *et al.* 1991; Destexhe & Pare, 1999). In this concept individual synaptic inputs and their precise timing are of little significance for the cells' output pattern (Shadlen & Newsome, 1998).

The low rates of AP activity observed in whole-cell recordings could suggest, however, that responses of barrel cells to sensory stimuli are not necessarily the result of massive balanced synaptic inputs. The subthreshold responses may reflect superposition of relatively few, in the order of tens, unitary inputs locked precisely to the onset of deflection. We refer to this as a 'selective input' computation scheme. Under such conditions the precise timing of synaptic inputs determines postsynaptic output (Abeles, 1983; Zador, 1998).

Representation of tactile stimuli in barrels and septa

Barrel neuron ensembles are able to represent in their PSP pattern the fine spatial structure of stimuli and they are

also able to signal the exact time at which a particular whisker was deflected relative to other whiskers. The high temporal fidelity of barrel neuron responses could be particularly important in the context of the animal's rhythmic exploratory whisking behaviour (Welker, 1964; Carvell & Simons, 1990). Specifically barrel cells may signal, at what time point during the whisking epoch a particular whisker was deflected and thus contribute to the ability of the animal to discriminate between small differences in surface texture. Cells in septa do not respond well to single whisker stimuli and their responses have a low spatial and temporal resolution. The multi-whisker RFs of septum cells suggest that these cells might represent stimuli that deflect collectively several whiskers and it seems likely that septum cells integrate excitation evoked during multiple whisking cycles. Septum cell activity signals to other layers of cortex the coarse structure of the animals tactile environment, for example as to whether it is moving in a tunnel or next to a wall.

Thus already in the input layer of the cortex three anatomically defined classes of cells can represent different cues of the animals' tactile environment. It will be interesting to determine whether and how the representation of object cues is further elaborated in specific classes of neurons located in the supra- and infragranular somatosensory cortex.

REFERENCES

Abeles, M. (1983). Role of the cortical neuron: integrator or coincidence detector? *Israel Journal of Medical Sciences* **18**, 83–92.

Armstrong-James, M. (1995). The nature and plasticity of sensory processing within adult rat barrel cortex. In *The Barrel Cortex of Rodents*, ed. Jones, E. G. & Diamond, I. T., pp. 333–374. Plenum Press, New York.

Armstrong-James, M., Callahan, C. A. & Friedman, M. A. (1991). Thalamocortical processing of vibrissal information in the rat. Intracortical origins of surround but not centre receptive fields of layer IV neurons in rat S1 barrel field cortex. *Journal of Comparative Neurology* **303**, 193–210.

Armstrong-James, M., Diamond, M. E. & Ebner, F. F. (1994). An innocuous bias in whisker use in adult rats modifies receptive fields of barrel cortex neurons. *Journal of Neuroscience* **14**, 6978–6991.

Armstrong-James, M. & Fox, K. (1987). Spatio-temporal divergence and convergence in the rat 'barrel' cortex. *Journal of Comparative Neurology* **263**, 265–281.

Armstrong-James, M., Fox, K. & Das-Gupta, A. (1992). Flow of excitation within rat barrel cortex on striking a single vibrissa. *Journal of Neurophysiology* **68**, 1345–1358.

Arnold, P. B., Li, C. X. & Waters, R. S. (2001). Thalamocortical arbors extend beyond single cortical barrels: an *in vivo* tracing study in the rat. *Experimental Brain Research* **136**, 152–168.

Bernander, O., Douglas, R. J., Martin, K. A. & Koch, C. (1991). Synaptic background activity influences spatiotemporal integration in single pyramidal cells. *Proceedings of the National Academy of Sciences of the USA* **88**, 11569–11573.

Blanton, M. G., Lo Turco, L. L. & Kriegstein, A. R. (1989). Whole cell recording from neurons in slices of reptilian and mammalian cerebral cortex. *Journal of Neuroscience Methods* **30**, 203–210.

Borg-Graham, L. J., Monier, C. & Fregnac, Y. (1998). Visual input evokes transient and strong shunting inhibition in visual cortical neurons. *Nature* **393**, 369–373.

Brecht, M. & Sakmann, B. (2000). *In vivo* whole-cell recordings from identified neurons in the rat somatosensory thalamus and cortical layer IV. *Society for Neuroscience Abstracts* **26**, 2106.

Brecht, M. & Sakmann, B. (2002). Whisker maps of neuronal subclasses in the rat ventral posterior medial thalamus, identified by whole-cell voltage recording and morphological reconstruction. *Journal of Physiology,* **538**, 495–515.

Carvell, G. E. & Simons, D. J. (1988). Membrane potential changes in rat SmI cortical neurons evoked by controlled stimulation of mystacial vibrissae. *Brain Research* **448**, 186–191.

Carvell, G. E. & Simons, D. J. (1990). Biometric analyses of vibrissal tactile discrimination in the rat. *Journal of Neuroscience* **10**, 2638–2648.

Chmielowska, J., Carvell, G. E. & Simons D. J. (1989). Spatial organization of thalamocortical and corticothalamic projection systems in the rat SmI barrel cortex. *Journal of Comparative Neurology* **285**, 325–338.

Destexhe, A. & Pare, D. (1999). Impact of network activity on the integrative properties of neocortical pyramidal neurons *in vivo*. *Journal of Neurophysiology* **81**, 1531–1547.

Diamond, M. E. (1995). Somatosensory thalamus of the rat. In *The Barrel Cortex of Rodents*, ed. Jones, E. G. & Diamond, I. T., pp. 189–219. Plenum Press, New York.

Diamond, M. E., Armstrong-James, M. & Ebner, F. F. (1992). Somatic sensory responses in the rostral sector of posterior group (PoM) and in the ventral posterior medial nucleus (VPM) of the rat thalamus. *Journal of Comparative Neurology* **318**, 462–476.

Diamond, M. E, Armstrong-James, M. & Ebner, F. F. (1993). Experience-dependent plasticity in the barrel cortex of adult rats. *Proceedings of the National Academy of Sciences of the USA* **90**, 2602–2606.

Dykes, R. & Lamour, Y. (1988). Neurons without demonstrable receptive fields outnumber neurons having receptive fields in samples from the somatosensory cortex of anesthetized or paralyzed cats and rats. *Brain Research* **440**, 133–143.

Elston, G. N., Pow, D. V. & Calford, M. B. (1997). Neuronal composition and morphology in layer IV of two vibrissal barrel subfields of rat cortex. *Cerebral Cortex* **7**, 422–431.

Feldmeyer, D., Egger, V., Lübke, J. & Sakmann, B. (1999). Reliable synaptic connections between pairs of excitatory layer 4 neurones within a single 'barrel' of developing rat somatosensory cortex. *Journal of Physiology* **521**, 169–190.

Friedberg, M. H., Lee, S. M. & Ebner, F. F. (1999). Modulation of receptive field properties of thalamic somatosensory neurons by the depth of anaesthesia. *Journal of Neurophysiology* **81**, 2243–2252.

Goldreich, D., Kyriazi, H. T. & Simons, D. J. (1999). Functional independence of layer IV barrels in rodent somatosensory cortex. *Journal of Neurophysiology* **82**, 1311–1316.

Hartings, J. A. & Simons, D. J. (1998). Thalamic relay of afferent responses to 1- to 12-Hz whisker stimulation in the rat. *Journal of Neurophysiology* **80**, 1016–1019.

Hines, M. L. & Carnevale, N. T. (1997). The NEURON simulation environment. *Neural Computation* **9**, 1179–1209.

Horikawa, K. & Armstrong, W. E. (1988). A versatile means of intracellular labeling: injection of biocytin and its detection with avidin conjugates. *Journal of Neuroscience Methods* **25**, 1–11.

Huang, W., Armstrong-James, M., Reama, V., Diamond, M. E. & Ebner, F. F. (1998). Contribution of supragranular layers to sensory processing and plasticity in adult rat barrel cortex. *Journal of Neurophysiology* **80**, 3261–3271.

Ito, M. (1988). Response properties and topography of vibrissa-sensitive neurons in the rat. *Journal of Neurophysiology* **60**, 1181–1197.

Ito, M. (1992). Simultaneous visualization of cortical barrels and horseradish peroxidase injected layer 5b vibrissa neurons in the rat. *Journal of Physiology* **454**, 247–265.

Kim, U. & Ebner, F. F. (1999). Barrels and septa: separate circuits in rat barrels field cortex. *Journal of Comparative Neurology* **408**, 489–505.

Koralek, K. A., Jensen, K. F. & Killackey, H. P. (1988). Evidence for two complementary patterns of thalamic input to the rat somatosensory cortex. *Brain Research* **463**, 346–351.

Lorente De No, R. (1922). La corteza cerebral del raton. *Trab. Lab. Investis. Biol. Madrid* **20**, 41–78.

Lu, S. M. & Lin, R. C. (1993). Thalamic afferents of the rat barrel cortex: a light- and electron-microscopic study using *Phaseolus vulgaris* leucoagglutinin as an anterograde tracer. *Somatosensory and Motor Research* **10**, 1–16.

Lübke, J., Egger, V., Sakmann, B. & Feldmeyer, D. (2000). Columnar organization of dendrites and axons of single and synaptically coupled excitatory spiny neurons in layer 4 of the rat barrel cortex. *Journal of Neuroscience* **20**, 5300–5311.

Margrie, T. W., Brecht, M. & Sakmann, B. (2002). *In vivo* low resistance whole-cell recordings from neurons in the awake and anaesthetized and awake mammalian brain. *Pflügers Archiv* (in the Press).

Martin, K. A. C. & Whitteridge, D. (1984). Form, function and intracortical projections of spiny neurons in the striate visual cortex of the cat. *Journal of Physiology* **353**, 463–504.

Moore, C. I. & Nelson, S. B. (1998). Spatio-temporal subthreshold receptive fields in the vibrissa representation of rat primary somatosensory cortex. *Journal of Neurophysiology* **80**, 2882–2892.

Petersen, C. C. & Sakmann, B. (2000). The excitatory neuronal network of rat layer 4 barrel cortex. *Journal of Neuroscience* **20**, 7579–7586.

Petersen, C. C. & Sakmann, B. (2001). Functionally independent columns of rat somatosensory barrel cortex revealed with voltage-sensitive dye imaging. *Journal of Neuroscience* **21**, 8435–8446.

Petersen, R. S. & Diamond, M. E. (2000). Spatial-temporal distribution of whisker-evoked activity in rat somatosensory cortex and the coding of stimulus location. *Journal of Neuroscience* **15**, 6135–6143.

Pinto, D. J., Brumberg, J. C. & Simons, D. J. (2000). Circuit dynamics and coding strategies in rodent somatosensory cortex. *Journal of Neurophysiology* **83**, 1158–1166.

Ramon y Cajal, S. (1893). *Nuevo Concepto de la Histologia de los Centros Nerviosos.* Barcelona.

Reyes, A., Lujan, R., Rozov, A., Burnashev, N., Somogyi, P. & Sakmann, B. (1998). Target-cell-specific facilitation and depression in neocortical circuits. *Nature Neuroscience* **4**, 279–285.

Rozov, A. , Burnashev, N., Sakmann, B. & Neher, E. (2001). Transmitter release modulation by intracellular Ca^{2+} buffers in facilitating and depressing nerve terminals of pyramidal cells in layer 2/3 of the rat neocortex indicates a target cell-specific difference in presynaptic calcium dynamics. *Journal of Physiology* **531**, 807–826.

Shadlen, M. N. & Newsome, W. T. (1998). The variable discharge of cortical neurons: implications for connectivity, computation, and information coding. *Journal of Neuroscience* **18**, 3870–3896.

Simons, D. J. (1978). Response properties of vibrissa units in rat SI somatosensory neocortex. *Journal of Neurophysiology* **41**, 798–820.

Simons, D. J. (1983). Multi-whisker stimulation and its effects on vibrissa units in rat SmI barrel cortex. *Brain Research* **276**, 178–182.

Simons, D. J. (1985). Temporal and spatial integration in the rat SI vibrissa cortex. *Journal of Neurophysiology* **54**, 615–635.

Simons, D. J. (1995). Neuronal integration in the somatosensory whisker/barrel cortex. In *The Barrel Cortex of Rodents*, ed. Jones, E. G. & Diamond, I. T., pp. 262–298. Plenum Press, New York.

Simons, D. J. & Carvell, G. E. (1989). Thalamocortical response transformations in the rat vibrissa/barrel system. *Journal of Neurophysiology* **61**, 311–330.

Simons, D. J., Carvell, G. E., Hershey, A. E. & Bryant, D. P. (1992). Responses of barrel cortex neurons in awake rats and effects of urethane anesthesia. *Experimental Brain Research* **91**, 259–272.

Simons, D. J. & Woolsey, T. A. (1984). Morphology of Golgi-cox impregnated barrel neurons in rat SmI cortex. *Journal of Comparative Neurology* **230**, 119–232.

Waite, P. M. E. (1973). Responses of cells in the rat thalamus to mechanical movements of the whiskers. *Journal of Physiology* **228**, 541–561.

Welker, C. (1976). Receptive fields of barrels in the somatosensory neocortex of the rat. *Journal of Comparative Neurology* **166**, 173–189.

Welker, W. I. (1964). Analysis of sniffing of the albino rat. *Behaviour* **22**, 223–244.

Woolsey, T. A., Dierker, M. L. & Wann, D. R. (1975). Mouse SmI cortex: Qualitative and quantitative classification of Golgi-impregnated barrel neurons. *Proceedings of the National Academy of Sciences of the USA* **72**, 2165–2169.

Woolsey, T. A. & Van Der Loos, H. (1970). The structural organization of layer IV in the somatosensory region (SI) of mouse cerebral cortex. The description of a cortical field composed of discrete cytoarchitectonic units. *Brain Research* **17**, 205–242.

Wong-Riley, M. (1979). Changes in the visual system of monocularly sutured or enucleated cats demonstratable with cytochrome oxidase. *Brain Research* **171**, 11–28.

Zador, A. (1998). Impact of synaptic unreliability on the information transmitted by spiking neurons. *Journal of Neurophysiology* **79**, 1219–1229.

Zhu, J. J. & Connors, B. W. (1999). Intrinsic firing patterns and whisker-evoked synaptic responses of neurons in the rat barrel cortex. *Journal of Neurophysiology* **81**, 1171–1183.

Acknowledgements

We would like to thank Troy Margrie for technical advice, Fritjof Helmchen, Troy Margrie, Carl Petersen, Nathan Urban and Jack Waters for comments on the manuscript. Marlies Kaiser, Rolf Rödel, Peter Mayer and Karl Schmidt provided excellent technical assistance. Arnd Roth kindly provided help with the 2D display of 3D cell reconstructions and calculation of contour lines as well as RF density plots. We are grateful for the help of Andreas Krauß and Laleh Sinai-Esfahani in cell staining and reconstruction.